Journal of Tissue Engineering
Volume 14: 1–21

DOI: 10.1177/20417314231197793
journals.sagepub.com/home/tej
Sage

3D bioprinting of corneal models: A review of the current state and future outlook

Leon Balters and Stephan Reichl

Abstract

The cornea is the outermost layer of the eye and serves to protect the eye and enable vision by refracting light. The need for cornea organ donors remains high, and the demand for an artificial alternative continues to grow. 3D bioprinting is a promising new method to create artificial organs and tissues. 3D bioprinting offers the precise spatial arrangement of biomaterials and cells to create 3D constructs. As the cornea is an avascular tissue which makes it more attractive for 3D bioprinting, it could be one of the first tissues to be made fully functional via 3D bioprinting. This review discusses the most common 3D bioprinting technologies and biomaterials used for 3D bioprinting corneal models. Additionally, the current state of 3D bioprinted corneal models, especially specific characteristics such as light transmission, biomechanics, and marker expression, and in vivo studies are discussed. Finally, the current challenges and future prospects are presented.

Keywords

3D bioprinting, cornea, eye, tissue engineering, regenerative medicine

Date received: 13 June 2023; accepted: 13 August 2023

Introduction

Based on a meta-analysis by Flaxman et al. that was published in the Lancet in 2017, it was estimated that by 2020, there may be more than 4.3 million cases of corneal blindness and moderate or severe vision impairments worldwide due to corneal opacity alone. Furthermore, corneal opacity cases were also projected to increase from 2015 to 2020. In addition, trachoma, which is an infection of the cornea, is one of the six most common causes of blindness, along with corneal opacity.[1] The World Health Organization (WHO) proposed that trachoma could be eliminated by 2020 through the SAFE strategy, which includes surgery for entropion and trichiasis, antibiotics for infectious trachoma, facial cleanliness to reduce transmission, and environmental improvements.[2,3] Although cases of trachoma have been reduced, it is still a relevant cause of corneal blindness.[1] Corneal blindness and corneal visual impairment have a greater impact on younger people and result in a very high proportion of disability-adjusted life years compared with the most common cause of blindness (cataracts).[4] Most cases of corneal blindness are preventable. For example, keratomalacia can be prevented with extensive vitamin A supplementation through dietary changes or food fortification to avoid malnutrition.[5] However, if corneal disease is too severe and medical treatment does not elicit improvement, a partial or full corneal transplant (keratoplasty) can restore visual function.[6] The indications for keratoplasty vary among regions. In the United States, the most common indications for corneal transplantation are Fuchs endothelial dystrophy, pseudophakic bullous keratopathy, and keratoconus, whereas worldwide, keratoconus and keratitis, for example, due to trachoma, are the most common indications.[7] Penetrating keratoplasty (PKP) is the surgery of choice in most areas of the world. Due to the different indications for the United States, more specific keratoplasty, such as

Institute of Pharmaceutical Technology and Biopharmaceutics, Technische Universität Braunschweig, Braunschweig, Germany

Corresponding author:
Stephan Reichl, Institute of Pharmaceutical Technology and Biopharmaceutics, Technische Universität Braunschweig, Mendelssohnstraße 1, Braunschweig 38106, Germany.
Email: s.reichl@tu-braunschweig.de

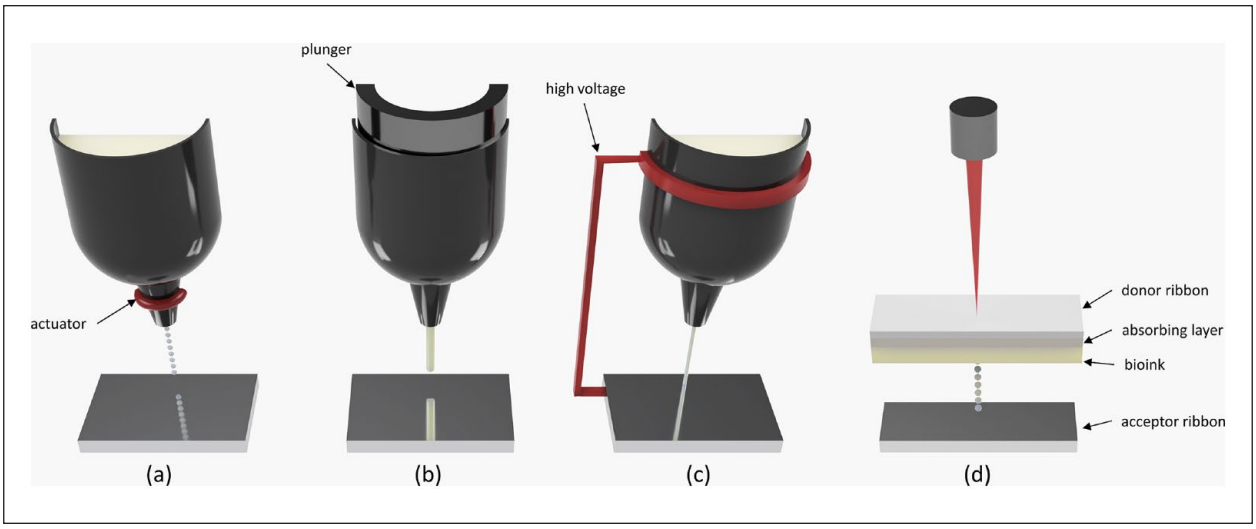

Figure 1. (a) Drop-on-demand printers use an actuator (e.g. thermal or piezoelectric) to create vapor bubbles that lower the surface tension, resulting in the release of drops of bioink, (b) extrusion printers utilize pressure, which can be applied with a plunger, to extrude the bioink, (c) meltelectrowriting uses high voltage between the cartridge or the nozzle onto a grounded collector to conduct the ink onto it, and (d) laser-assisted: a laser pulse hits the donor ribbon (glass) and the absorbing layer (e.g. titanium or gold), which causes a brief heating of the bioink ribbon and subsequently causes the release of droplets on the acceptor ribbon.

endothelial keratoplasty (EK) and anterior lamellar keratoplasty (ALK), as well as deeper anterior lamellar keratoplasty (DALK), are more common in this area.[8] Although human corneas are the most commonly transplanted tissue throughout the world, there is an immense shortage of corneal donors worldwide, thus resulting in only one in 70 people receiving a corneal transplant.[9,10]

Bioprinting can fulfill the aforementioned needs for artificial corneas.[11] Bioprinting is an additive manufacturing process that involves computer-aided design (CAD), as well as the patterning and assembly of biomaterials or bioinks. It is mainly used in regenerative medicine, along with pharmacokinetic and cell studies.[12,13] Bioprinted artificial corneas can have advantages over current tissue engineered artificial corneas. For example, the spatial arrangement of the material can lead to improved geometry and enhanced physical properties compared to conventional tissue engineering.[14]

Only 2% of worldwide bilateral corneal blindness affects developed countries.[4] In addition, the shortage of cornea donors is mainly localized in the least developed countries.[10] Bioprinting could be a technology that has the potential to demonstrate high-throughput capabilities and still be cost-effective. Another value of bioprinted corneas is their use in in vitro drug screening. In vitro tests are mandatory in preclinical studies. Moreover, current cell culture models of the human cornea cannot predict the behavior of drugs as precisely as in the physiological environment.[15] Improved 3D models could also be beneficial in this scenario.[16]

In this review, the most commonly used bioprinting technologies and biomaterials for bioinks for corneas are presented and discussed. This discussion is followed by an evaluation of the current state of printed corneas, focusing on key functions such as cell viability, light transmission, biomechanical properties, expression of specific proteins and genes, and swelling and degradation of bioprinted corneas. In addition, an evaluation of the in vivo studies that have been conducted to date is explained. This discussion leads to outlooks and future perspectives, as well as ethical concerns that may be relevant.

Bioprinting technologies

3D printing originated in the 1980s with stereolithography (SLA).[17,18] Although this technology was not used in the bioprinting field at that time, it has recently been used for the bioprinting of corneal stromal tissue.[19,20] SLA is based on photopolymerization of a liquid resin bath to solidify objects with a laser light source.[21] A similar technology that uses a projector light source, which is known as digital light processed printing (DLP), has also been recently used in cornea bioprinting.[22–24] These are only two of the many technologies that have been developed in recent years. The most common technique is extrusion, followed by drop-on-demand and laser-assisted technologies. An overview of the most common techniques can be seen in Figure 1.

First, to be able to print, a digital model is needed. A digital model can be based on computed tomography, magnetic resonance imaging, or X-ray scans.[25,26] These data can be converted through a CAD program into a viable CAD model. Another option is to create the digital object in a CAD program itself. These files are then formatted into a fabrication code, which is often known as

g-Code. The fabrication codes are the instructions for the printer to execute the printing process.[27] Native corneas do possess a curvature that is currently difficult to recreate with conventional tissue engineering. Therefore, the bioprinting of a 3D model wherein the curvature is already implemented is an important advantage of bioprinting.[22]

Extrusion

Extrusion is the most widely applied technology because it is inexpensive and easily obtainable.[28] Therefore, it is also the most commonly used technology for corneal bioprinting.[20,22,26,29–36] The basic principle of extrusion printing is to apply pressure to a cartridge to continuously dispense the material through a nozzle. Pressure can be applied by using pneumatic or mechanical force.[25] The advantage of extrusion printing is the possible higher throughput. For example, a procedure lasting less than 10 min for one cornea was achieved.[20] Another advantage is the possibility of printing a wide range of materials with high viscosities.[25] The ability to print high viscosities indicates that high cell density can also be printed. In corneal application, cell densities of up to 5 million per ml could be printed.[32]

Although extrusion bioprinting can have negative effects on cell viability due to shear stress when extruded through the nozzle, this was not the case for bioprinted corneal models.[25,37] Most of the conducted studies have demonstrated high cell viability. This could be due to the efficient use of appropriate bioinks and nozzle sizes.[20] Another disadvantage of extrusion printing is the clogging of the print head, which occurs with highly viscous bioinks and depends on the size of the nozzle and the extrusion force. Another influence may be the high cell density and the rapid adhesion of cells.[38] Until now, clogging has not been described in corneal bioprinting.

Drop-on-demand (DoD)

Drop-on-demand, which is also often referred to as inkjet-based or droplet-based, is a technology that was developed in the 1950s and commercialized in the 1970s by Siemens. However, the first inkjet printer capable of 3D printing was developed in 2000.[39] A modification of the inkjet printing system led to the dispensing of proteins and cell solutions.[40] There are many different technologies for performing drop-on-demand printing. The most common technologies are thermal inkjet, piezoelectric inkjet, acoustic inkjet, microvalve inkjet, electrohydrodynamic, and electrostatic inkjet.[39,41] Microvalve inkjet involves a nozzle. Thus, it can be prone to nozzle clogging. Additionally, the implantation of a bioink with fitting properties is crucial for microvalve inkjets.[38] Although it is a widely applied technology, only one group has been able to utilize the electromagnetic microvalve inkjet to bioprint corneal stromas.[42] Duarte Campos et al. achieved their aims of high cell viability, optical transmission, and positive expression of keratocan and lumican in human cornea stroma keratocytes. One disadvantage of inkjet bioprinting is the long production time. Duarte Campos et al. needed 1 h to create their model, which did not reflect the size of a native cornea.[42] Another group used aerosol jet printing, which is a method that is normally used for electronic printing. This method provides a very high resolution that cannot be achieved via extrusion printing. Moreover, Gibney et al. were able to print an acellular stromal model of a few hundred μm thickness. Similar to Duarte Campos et al., they required at least 4 h for the printing process. Another disadvantage of aerosol printing is that no cells can come into direct contact with the ink.[43] Thus, a combination with another printing method could solve the issue of direct cooperation of cells in the scaffold.

Laser-assisted

The first application of laser-assisted printing in bioprinting occurred in 2004, wherein human osteosarcoma cells were printed in a 3D layer.[44] Laser-assisted bioprinting is often based on laser-induced forward transfer (LIFT).[25] To the best of our knowledge, LIFT has only been utilized once in cornea bioprinting.[45] LIFT is more complex than the aforementioned technologies.[46] Specifically, it consists of a laser beam that is guided via a focusing lens onto a donor ribbon made of glass. The bioink is linked to the donor ribbon. Between the donor ribbon layer and the bioink layer, there can be an absorbing layer made of metals (e.g. gold or titan) or biopolymers.[25,47] The energy of the laser is subsequently converted into heat by the donor ribbon. This scenario leads to evaporation bubbles, which then emit droplets or jets of bioink onto the acceptor ribbon.[48] LIFT bioprinting can achieve a higher resolution and printing accuracy than inkjet or extrusion bioprinting. Furthermore, because it is a nozzle-free printing technology, nozzle clogging with high viscosity materials cannot occur in LIFT bioprinting.[49] Therefore, high cell densities of up to 8 million cells per ml are possible.[25] Furthermore, LIFT bioprinting exerts less shear stress on the cells due to the nozzle-free technology, which subsequently leads to high viability of the cells. Sorkio et al. not only demonstrated high resolution in cornea bioprinting, but also showed high cell viability.[45] The drawbacks of laser-assisted bioprinting include its high cost and low printing efficiency compared to inkjet or extrusion printing.[49]

Electrospinning and (melt-)electrowriting

Electrowriting and electrospinning are based on the same physics. When a high voltage between a cartridge and a grounded collector, fibers can be deposited onto the collector bed from the tip of the cartridge. Although electrospinning possesses a whipping of the fiber jet that leads to the

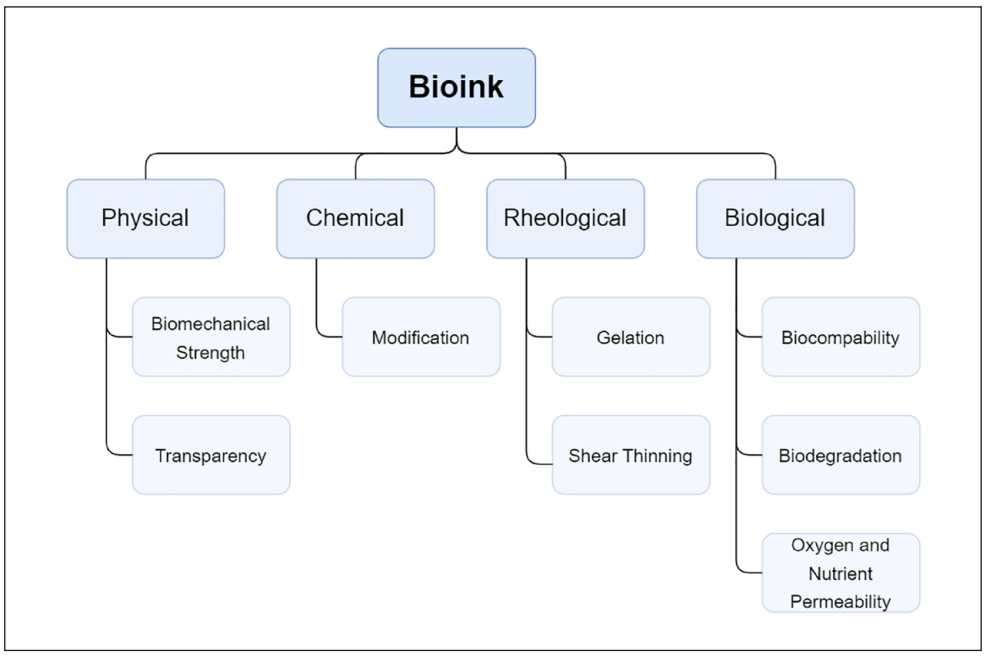

Figure 2. Requirements of bioink for corneal bioprinting.

deposition of meshes, electrowriting is able to directly deposit the fiber in a linear way. Additionally, electrowriting mainly uses polymers such as polycaprolactone, which are melted; hence, the common name of this technology is melt electrowriting.[50] Electrospinning has been extensively used in the field of corneal tissue engineering, as it produces tissues that supposedly resemble native ECM, thereby showing promising results.[51] However, it is suggested that the type of collagen extraction plays a pivotal role in creating the ultrastructure of collagen with electrospinning.[52] Research has shown that electrospun collagen fibers are not able to represent native structures due to the lack of refolding of collagen fibers.[53] For further research in terms of electrospinning and corneal tissue engineering, the review written by Kong and Mi[51] is recommended. Furthermore, a hybrid fabrication method combining melt electrowriting followed by perfusion of a bioink was proposed by Kong et al.[54]

Light-based technologies

The aforementioned SLA and DLP technology can be categorized into vat-polymerization. These techniques require a photoinitiator that is often cytotoxic.[55] Furthermore, the biocompatibility of the biomaterial is currently poor.[21] Thus, these techniques are limited to printing with cells. However, SLA and DLP have been used to print corneal support scaffolds.[19,20,22] Due to the dome-shaped geometry of corneas, a support scaffold may be helpful to achieve the unique curvature of the cornea. Nevertheless, the latest research has demonstrated an increase in light-based technologies for bioprinting applications.[56] Mahdavi et al. were able to apply stereolithography with human corneal stromal cells and demonstrated a feasible cell viability of 81% on day 1 by using a 2,5-diphenyltetrazolium bromide (MTT) assay.[19] Most recently, He et al. were able to DLP bioprint a two-layered corneal model consisting of an epithelial and stromal layer with a high cell viability of 90%.[24] Additionally, Zhong et al. achieved similar high cell viability with DLP printing of a combined bioink consisting of GelMA and glycidyl methacrylate hyaluronic acid (HAGM).[23]

Bioinks and biomaterial ink

Bioinks play a crucial role in creating a viable bioprinted model. Bioinks are essential components of the bioprinting process. According to Groll et al., bioinks must contain cells to be defined as bioinks. Bioinks are not made solely from cells; instead, they are accompanied by biomaterials.[57] Biomaterials can be naturally or synthetically derived. Naturally derived biomaterials are often used because they share more similarities with the extracellular matrix (ECM) of human tissue.[58] This also applies for cornea bioprinting. Common natural biomaterials include collagen, gelatin, methacrylated gelatin (GelMA), alginate, chitosan, hyaluronic acid, agarose, and cellulose.[59–65] Except for cellulose, all of these biomaterials have been applied in cornea bioprinting (Figure 3). Synthetic biomaterials can include polyethylene glycol (PEG), pluronic, polylactic acid (PLA), polycaprolactone (PCL), and polylactic-coglycolic acid (PLGA).[66–71] Furthermore, certain requirements must be met in bioinks to make them suitable for cornea bioprinting (Figure 2). These properties include

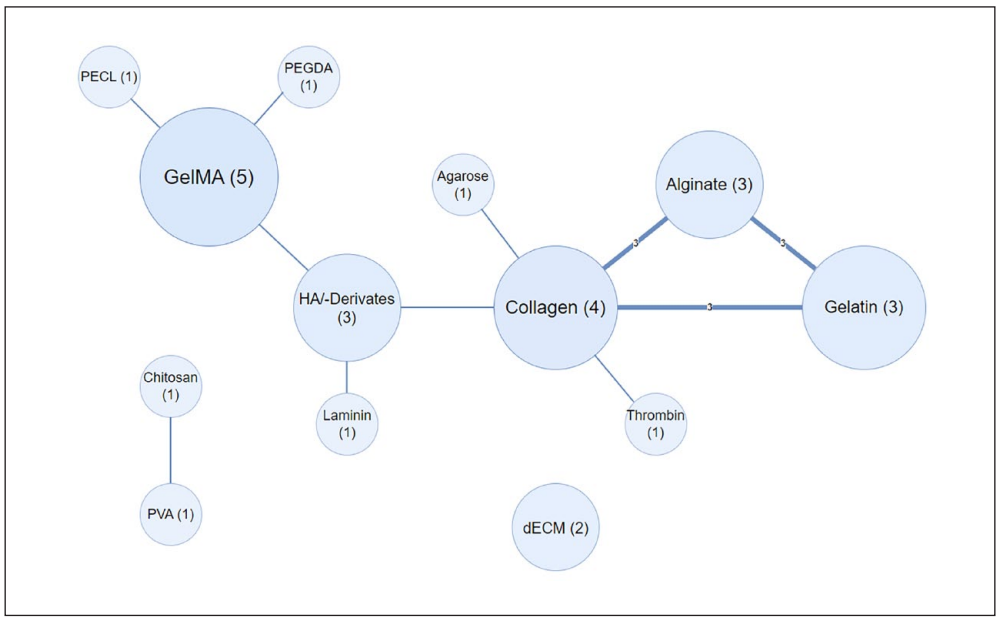

Figure 3. Overview of biomaterials used in corneal bioprinting. PVA: polyvinylalcohol, HA/-derivates: hyaluronic acid, also including HAGM: hyaluronic acid glycidyl meth-acrylate and HA-CDH: hyaluronic acid carbodihydrazide, dECM: decullarized extracellular matrix, and PECL: poly (ε-capro-lactone)-poly (ethylene glycol).

sufficient biomechanical strength, transparency, biocompatibility, and encouraging high cell viability, as well as cell morphology, which allows the proper expression of specific proteins.[72] To achieve better biomechanical strength, combinations of two or more different biomaterials have been applied (Figure 3).[20] In addition, bioinks must be printable (i.e. they must have shear-thinning viscosity and an efficient gelation process for extrusion printing). For gelation, crosslinking is a key process to maintain the 3D printed structure. Various methods of crosslinking exist, with chemical and physical crosslinking being the most common types.[73] The crosslinking method that is used depends on various factors. These factors can involve the biomaterial itself and the respective mechanical stiffness of the cornea model. Moreover, the bioink must biodegrade so that the cells themselves can form their own extracellular matrix in a manner in which the construct still supports itself. Finally, as in 2D models, cells require oxygen and nutrients, which are often provided by the medium. Therefore, the bioink must be permeable to oxygen and nutrients so that even the cells that are farthest from the surface are preserved. To achieve all of these requirements, it is common to chemically modify the material, such as through the cooperation of methacrylate in biomaterials.

Collagen

Collagen (more specifically, type I collagen) is the most abundant protein in the ECM of corneas.[74] Therefore, most bioprinted cornea models have used collagen as the main component of bioprinting.[20,26,29,42,43,45] The advantages of collagen include low immunological reactions and increased cell growth, adhesion, and attachment due to being a triple helical biocompatible protein with an RGD (arginine-glycine-aspartic acid) motif.[75] The disadvantage of using only collagen as a bioink is the low mechanical strength and slow gelation time, which requires up to 30 min at 37°C.[55] Thus, as an example, chemical modification with methacrylate can increase mechanical strength.[26] Another possibility is to combine collagen with other biomaterials, such as gelatin and alginate used by Kutlehria et al.,[20] as well as Wu et al.,[29] to increase mechanical strength. Another example originates from Duarte Campos et al. Specifically, they used collagen in combination with agarose to further increase the robustness. However, the bioink of Duarte Campos et al. had significantly lower mechanical properties than human corneal tissue.[42] Therefore, the bioink proposed by Duarte Campos et al. is not suitable for cornea bioprinting and needs further improvements.

Gelatin and GelMA

Through the process of partial hydrolysis of collagen, gelatin can be obtained.[76] Therefore, gelatin has similar properties as collagen, including being biocompatible, transparent, and nontoxic, as well as exhibiting improved cell attachment through the RGD motif.[34] Furthermore, gelatin can gel more easily than collagen and is thereby more suitable for extrusion bioprinting, as the construct needs to be self-supporting.[29] In addition to collagen, gelatin has less antigenicity and better solubility.[77] However,

gelatin (similar to collagen) lacks mechanical stability; therefore, it needs to be further modified and enhanced for implementation in bioprinting.[77,78] Additionally, gelatin needs to be cooled to reach its gel state, which can affect cell viability.[79] To address the aforementioned problems, there are two different solutions: first, gelatin can be combined with other biomaterials, and second, gelatin can be modified, for example, by attaching methacrylate to GelMA, which can be easily crosslinked via exposure to UV light.[19,20,22–24,29,34,54] Zhang et al. demonstrated the integration of GelMA for the support scaffold. Furthermore, they implemented gelatin and alginate at concentrations of 0.10 and 0.02 g/mL, respectively, as the main components of the bioink in combination with human corneal epithelial cells.[22] Moreover, Mahdavi et al.[19] and Kilic Bektas and Hasirci[34] used only GelMA as the core component of their bioink. Kong et al. proposed electrospinning a scaffold by using a synthetic biomaterial, poly (ε-capro-lactone)-poly (ethylene glycol) (PECL), and GelMA. In addition to these scaffolds, Kong et al. seeded limbal stromal stem cells.[54] Nevertheless, GelMA does not have the same mechanical properties as native corneas. Thus, Sharifi et al. proposed an increase in the degree of methacrylation of gelatin by using glycidyl methacrylate, which resulted in gelatin-glycidyl-methacrylate (GELGYM). GELGYM has better mechanical properties than GelMA in terms of tensile strength and elasticity up to 10 times and 4 times, respectively.[77] GELGYM could be a viable alternative to the currently most commonly used GelMA. Another viable option was proposed by He et al., who combined GelMA with a synthetic material known as poly(ethylene glycol) diacrylate (PEGDA) to further increase the toughness of the printed scaffold.[24]

Alginate

Alginate is a polysaccharide consisting of ß-D mannuronic acid and α-L-guluronic acid. The content of the individual monomer varies depending on the type and part of the algae from which it is obtained.[80] A higher content of α-L-guluronic acid results in a higher gel formation, whereas a higher content of ß-D-mannuronic acid increases the flexibility of the gel. Alginate has high biocompatibility, is biodegradable, and is nonimmunogenic.[81] Furthermore, it is inexpensive, making it one of the most widely used biomaterials for bioprinting.[58] Divalent cations are needed for the gelation process, with Ca^{2+} being the most commonly used, although it has a higher affinity for Sr^{2+} and Ba^{2+}.[82] To increase the long-term stability of alginate hydrogels, Ba^{2+} ions have been utilized.[83] A major disadvantage of alginate includes its slow degradation, which often leads to poor cell proliferation. Therefore, Wu et al. demonstrated the use of citrate to initiate controllable degradation, thus leading to a higher proliferation rate.[29] Another disadvantage of alginate is poor cellular adhesion due to the lack of the RGD motif. Thus, the combination with other biomaterials, such as collagen, is common.[20,22,26]

Decullarized extracellular matrix

Decullarized extracellular matrix (dECM) is derived from native animal or human tissue via physical, chemical, or biological processes.[84] It consists of a wide variety of components, the most common and important of which are collagen, glycosaminoglycans (GAGs), and growth factors.[85] One of the main advantages of dECM-bioink involves its higher biosimilarity to native tissue than other biomaterials. Therefore, Kim et al. created cornea-derived dECM (Co-dECM) from bovine eyeballs via chemical treatment with Triton X-100.[31] The use of Triton-X-100 can reduce the content of GAG.[86] In relation to the original tissue, the Co-dECM bioink of Kim et al. possessed $76.50 \pm 0.043\%$ GAG and $62.08 \pm 0.034\%$ collagen. Furthermore, there was a discrepancy between the different amounts of growth factor between Co-dECM and the native cornea. For example, the amount of transforming growth factor (TGFa) and insulin-like growth factor (IGF-1) was 3.5 and 1.8 times lower, respectively, in Co-dECM than in the native cornea. However, the Co-dECM bioink of Kim et al. showed greater similarity with native corneas than collagen with native corneas in terms of growth factors and cytokines.[31]

Chitosan

Chitosan is obtained via the deacetylation of chitin, which is extracted from the exoskeleton of arthropods and the shells of crustaceans. It is a polysaccharide composed of n-acetyl d-glucosamine and d-glucosamine.[87] In tissue engineering, chitosan has been used due to its biocompatibility, antimicrobial activity, low toxicity and immunogenicity, and nontoxic biodegradability.[88] However, chitosan has poor mechanical properties and is subject to rapid degradation.[89] Ulag et al. demonstrated the use of chitosan in combination with polyvinyl alcohol for the bioprinting of an artificial cornea model.[33]

Hyaluronic acid

Hyaluronic acid (HA) is one of the most common components of the extracellular matrix.[90] It is also one of the most commonly used biomaterials in bioprinting.[58] However, under normal conditions, HA is not found in corneas.[91] Furthermore, HA is limited in corneal tissue engineering (including bioprinting) due to its association with lymphangiogenesis in the limbus; however, this requires further investigation.[92] Nevertheless, Sorkio et al. implemented 17% of 1% (w/v) HA in combination with human recombinant laminin, which is the main component of its bioink. However, Sorkio et al. did not explicitly state

why they additionally used HA.[45] Zhong et al. modified HA with glycidyl methacrylate (HAGM) to compare it with GelMA. They demonstrated that limbal stem cells can be quiescent within HAGM constructs and activated within GelMA constructs.[23] A different modification was performed by Mörö et al.; specifically, they utilized click chemistry and modified HA with carbodihydrazide (HA-CDH), as well as HA-CDH with dopamine and HA with aldehyde. To increase cytocompatibility, they added type I collagen to each bioink. In total, they used two different bioinks, with the first one consisting of HA-CDH with HA-aldehyde and collagen and the second bioink consisting of HA-CDH-dopamine with HA-aldehyde and collagen.[36]

Agarose

Similar to alginate, agarose is also obtained from marine seaweed. It is a polysaccharide consisting of ß-D-galactose and 3,6-anhydro-L-galactopyranose.[93] Agarose is one of the less common biomaterials for bioprinting.[58] This could be due to the fact that agarose supports cell growth to a limited extent.[94] Furthermore, the degradation of agarose is fairly slow; thus, additives such as ß-agarase can be useful to speed up the degradation.[95] However, agarose does not require crosslinking agents, as it can be thermally crosslinked, thereby providing mechanical stability to the bioprinted construct.[42,64]

Applications

Corneal anatomy and cell types

The human cornea is located in the anterior region of the outermost part of the eye. The cornea has two main functions. First, the cornea, in combination with the tear film, is responsible for the inner parts of the eye as the first biological barrier. Second, the cornea mostly contributes to the refraction of light, thus allowing for efficient vision.

Data from 14 studies from four continents (containing at least biometric data for 1300 eyes) indicate that the cornea has an axial length of 23.49 ± 1.35 mm, a corneal radius of curvature of 7.69 ± 0.28 mm, and a horizontal diameter (white to white) of 11.80 ± 0.42 mm. The depth of the anterior chamber is 3.10 ± 0.47 mm, and the lens thickness is 4.37 ± 0.43 mm.[96] Moreover, the cornea is aspheric, as well as convex, and has a varying thickness from central to peripheral areas. The central thickness is in the range of 544 ± 38 µm, and the peripheral thickness is up to 22% thicker.[96,97] The outermost layer of the cornea is the epithelium. It consists of five to seven cell layers, which are derived from the surface ectoderm and are approximately 50 µm thick. At the peripheral end, there are up to 10 layers of cells.[98] The epithelium is not keratinized, and the cells migrate from the bottom layer to the surface. As a result, cells are consistently renewed; in addition, due to migration, the basal cells are large and columnar, whereas the cells closer to the surface and the tear film tend to be flattened.[74] Attached to the epithelium lies the Bowman layer, which is an acellular remnant of the stroma consisting of type I and V collagen, as well as proteoglycans.[98] At more than 80%, the corneal stroma constitutes the largest part of the cornea. It consists of three main components: keratocytes, lamellae, and proteoglycans.[99] Moreover, there are more than 200 distinct lamellae in the stroma.[100] The lamellae are composed of heterofibrils that contain mainly type I and type V collagen fibers. Other collagens, such as types VI, III, and XII, can also be found in the stroma.[101] Proteoglycans such as keratan, chondroitin, and dermatan sulfate stabilize the fibrils via the regulation of hydration.[102] Keratocytes are thought to act as a link between lamellae to hold lamellae in place.[74] Furthermore, keratocytes produce collagen, as well as other proteins such as glycosaminoglycans and metalloproteases, which are important for maintaining the ECM.[102] Keratocytes are located between the lamellae and are flat and broad cells with a dendritic morphology.[103] Between the stroma and the endothelium is the Descemet's membrane, which grows from a size of a few micrometres to 10 µm with age. Furthermore, the Descemet's membrane is an acellular layer that is mainly composed of type IV collagen and glycoproteins such as laminin and fibronectin. Posterior to the Descemet's membrane is the endothelium, which is a cellular monolayer. Endothelial cells are hexagonal in shape and exhibit high metabolic activity.[104] However, endothelial cells are not mitotically active, but by birth, a high reservoir can be observed.[74] The cell density of endothelial cells decreases during life by approximately 0.6% per year.[105]

To our knowledge, with two exceptions, cornea bioprinting has always involved the printing of a single layer of the cornea, such as the stroma or epithelium. Sorkio et al. and He et al. were the only groups that printed the stroma and epithelium.[24,45] Due to the fact that the stroma is obviously the thickest layer of the cornea, it is reasonable to assume that the stroma is the most printed layer of the cornea. Of the 16 research articles that were evaluated in this review, 12 articles focused on corneal stroma bioprinting, 5 articles focused on epithelial bioprinting, and only one article focused on endothelial bioprinting. Furthermore, Mörö et al. used pluripotent stem cell-derived neurons for the innervation of the periphery of their corneal model consisting of the stroma and epithelium.[36] An overview of all of the research articles and their specific studies can be found in Table 1.

Cell viability

For bioprinting, it is essential that cells survive after being printed. Thus, high cell viability is one of the key

Table 1. Comparison of applications of corneal bioprinting.

Cornea layer	Cell type	Technology	Ink composition	cell viability	Protein and gene expression	Light transmission	Biomechanical properties	Experimental method	Swelling degradation	Reference
Epithelium	HCECs	Extrusion	Alg/Col/Gel	94.6%	CK3	62.2% (630 nm)		In vitro		Wu et al.[29]
Epithelium Stroma	hESC-LESC +hASCs	Laser	Lam/HA Col/Tr	High (not quantified)	p63α, p40, CK3, CK15, Ki67, collagen-type I, VWF			In vitro	DEG: 50% (8 days)	Sorkio et al.[45]
Endothelium	HCEnC	Extrusion	Gel	High (not quantified)	Na^+K^+ ATPase, ZO-1, CD44, CD166 (in vivo)	High in vivo (not quantified)		Rabbits		Kim et al.[30]
Stroma	HCK	Extrusion	Alg/ColMA	83%–92% (day 1 and 7)				In vitro		Isaacson et al.[26]
Epithelium	HCECs	Extrusion	Alg/Gel	>80%		85%–94% (300–700 nm)	YM: 0.2 MPa TS: 0.22 MPa	In vitro	SW: 15% (24 h)	Zhang et al.[22]
Stroma	hTMSCs	Extrusion	dECM	Very high (not quantified)	collagen-type I, keratocan, αSMA, KERA, ALDH, ACTA 2	High (not quantified)		Rabbits and mice		Kim et al.[31,32]
Stroma	HCK	DoD	Col/Agar	High (not quantified)	keratocan, lumican, αSMA	High (not quantified)	YM: <0.02 MPa	In vitro		Duarte Campos et al.[42]
Stroma	hTMSCs	Extrusion	dECM					In vivo		Park et al.[35]
Stroma	hASCs	Extrusion	Chit/PVA	<90% (7 days)		<61% (400–800 nm)	TS: >8.94 MPa	In vitro	SW: >300% (7 days)	Ulag et al.[33]
Stroma	HCK	Extrusion	Alg/Gel/Col	86%–96% (day 7 and 14)	f-actin, fibronectin	75%–90% (300–700 nm)		In vitro		Kutlehria et al.[20]
Stroma	LSSCs	Electrowriting	PECL/GelMA	High (not quantified) (day 3)	vimentin, ALDH3A1, aquaporin 1, type VI collagen, thymocyte antigen 1	74.7% (500 nm)	YM: 0.012 MPa TS: 3.47 MPa	Rats	SW: 13.9% (24 h)	Kong et al.[54]
Stroma	HCK	Extrusion	GelMA	>95% (21 days)	type I and VI collagen, decorin, αSMA	>75%	YM: 0.02 MPa	In vitro	DEG: 8% (3 weeks)	Kilic Bektas and Hasirci[34]
Stroma	HCK	SLA	GelMA	81–>100% (day 1, 3, and 7)	type I collagen, lumican, keratan	80%–94% (450–800 nm)		In vitro		Mahdavi et al.[19]
Epithelium	rbLSCs/hLSCs	DLP	GelMA, HAGM	day 7: 86.7 ± 1.6% 92.1 ± 0.8% (gel, respectively)	Ki67, KRT14, PAX6, CD200, $P27^{KIPI}$, P63, BMI1, VANGL1, WNT5A, CTNNB1, KRT3, △NP63		YM: <0.014 kPa	In vitro		Zhong et al.[23]
Stroma		DoD	rhCol III			>87.5 ±6% (390–700 nm)	YM: 0.506 ± 0.173 MPa	In vitro	SW: 6.8 ± 1.6%	Gibney et al.[43]
Epithelium Stroma	rASCs, rCECs	DLP	GelMA/PEGDA	90% (days 1 and 3)	CK3, type I collagen, lumican, αSMA, ALDH3A1, keratocan, AQP1	82.5% (600 nm)	YM: 0.1007 MPa TS: 0.0822 MPa	In vivo	SW: ≈ 100% (not specified) DEG: ≲ 50% (not specified)	He et al.[24]
Stroma	hASC/hASC-CSK, hPSC-neurons	Extrusion	HA-CDH/HA-Ald/Col/HA HA-DA-CDH/ HA-Ald/Col/HA	>95% (day 1 and 7)	Ki67, lumican, type I and V collagen, αSMA, ALDH3A1, keratan sulfate, keratocan, vimentin, connexin 43,	71.9 ± 1.3% (400 mm) 94.1 ± 1.5% (700 mm)	YM: 0.0103 MPa	In vitro and ex vivo porcine	SW: not specified DEG: ≈ 20% (not specified)	Mörö et al.[36]

HCECs: human corneal epithelial cells; LESC: limbal epithelial stem cells; hASCs: human adipose tissue derived stem cells; HCK: human corneal keratocytes; hTMSCs: human turbinate-derived mesenchymal stem cells; LSSCs: limbal stromal stem cells; rbLSCs – rabbit limbal stem cells; hLSCs: human limbal stem cells; DoD: drop-on-demand; Alg: alginate; Col: collagen; rhCol III: recombinant human type III collagen; Gel: gelatin; HA: hyaluronic acid; HAGM: hyaluronic acid glycidyl methacrylate; HA-CDH: hyaluronic acid carbodihydrazide; HA-DA-CDH: dopamine-modified hyaluronic acid carbodihydrazide; HA-Ald: hyaluronic acid aldehyde; Tr: thrombin; Lam: laminin; ColMA: methacrylated collagen; dECM: decullarized extracellular matrix; Agar: agarose; Chit: chitin; PVA: polyvinylalcohol; PECL: poly caprolactone-poly ethylene glycol; CK3: Cytokeratin 3; p63α and p 40: corneal progenitor marker; CK15: cytokeratin 15; Ki67: proliferation marker; VWF : von Willebrand factor; ZO-1: zonula ocludens 1; CD44 and CD166: cluster of differentiation; αSMA: alpha-smooth muscle actin; KERA, ALDH, ALDH3A1, and ACTA2: keratocyte specific genes; △NP63: proliferation marker; KRT14, PAX6, and BMi1: LSC markers; CD200 and P27KIPI: LSC quiescent markers; VANGL1 and WNT5A: noncanonical WNT signaling pathway markers; CTNNB1: canonical WNT signaling pathway markers; KRT3: corneal epithelium differentiation marker; YM: Young's modulus; TS: tensile strength; SW: swelling; DEG: degradation.

indicators for functional bioprinting in general. Various methods have been employed for in vitro cell viability for corneal bioprinting. The most common method for determining cell viability in corneal bioprinting is double staining with calcein-acetoxymethyl ester (Calcein AM) for living cells in combination with ethidium homodimer or propidium iodide (PI) for dead cells. Wu et al. used human corneal epithelial cells (HCECs) for bioprinting. Specifically, they examined both cell viability and cell proliferation in relation to the effect of sodium citrate on the degradation of bioink consisting of gelatin, alginate, and collagen. The calculation of cell viability as a percentage was performed according to the number of cells stained green with calcein AM divided by the number of total cells. Wu et al. demonstrated a high cell viability of $94.6 \pm 2.5\%$. They showed that sodium citrate increased the proliferation rate by 15.4% from day 2 to day 8. In conclusion, Wu et al. not only showed high cell viability for their method but also demonstrated the positive impact of sodium citrate on cell proliferation.[29] The corneal construct with primary human corneal keratocytes (HCKs) developed by Isaacson et al. was also stained with calcein AM and ethidium homodimer 1 on day 1 and day 7. For the calculation, they used the same formula as stated by Wu et al. Cell viability was 92% on day 1 but decreased to 83% on day 7.[26] Similar to Isaacson et al., Kutlehria et al. also used HCKs and examined cell viability at day 7 and day 14. The calculation and analysis were the same as those used by Isaacson et al. Their results demonstrated that the cell viability measurements on days 1 and 14 were $96 \pm 5\%$ and $86 \pm 2\%$, respectively. Furthermore, Kutlehria et al. observed the cell growth rate with an Alamar assay. Again, there was a decrease in the growth rate from day 5 to day 14 from $101 \pm 9\%$ to $93.8 \pm 7\%$, respectively.[20] Both studies demonstrated a decrease in cell viability over time. This effect could be due to the slow degradation of the bioinks over time. A similar method was used by Kilic Bektas and Hasirci.[34] They demonstrated a cell viability of HCK of over 95% over the course of 3 weeks. In addition, cell proliferation was assessed with an alamar assay. However, no significant change in proliferation was detected. Likewise, Zhong et al. evaluated LSCs' viability after 7 days in GelMA and HEGM scaffolds, resulting in $86.7 \pm 1.6\%$ and $92.1 \pm 0.8\%$, respectively.[23] Moreover, Duarte Campos et al. used fluorescein diacetate and propidium iodide staining for cell viability of HCKs on days 1 and 7. They concluded that only a few cells died during the course of 7 days; however, they did not quantify their results.[42]

Another approach to evaluate the cell cytocompatibility of HCK was performed by Mahdavi et al. using an MTT assay on days 1, 3, and 7. The cytocompatibility was calculated as the absorbance of the bioprinted hydrogel divided by the absorbance of cells cultured on a culture plate as a percentage. On day 1, cytocompatibility was 81% and increased to over 100% on days 3 and 7. Thus, they demonstrated improved cell proliferation compared to their conventional 2D culturing method.[19] He et al. combined the MTT assay with live/dead staining (Calcein AM/PI) to evaluate cell cytotoxicity and cell viability with both methods and observed high cell viability, with more than 90% viability observed on days 1 and 3.[24] Furthermore, Ulag et al. also used an MTT assay to evaluate the cell viability of human adipose-derived stem cells (hASCs) differentiated into HCKs. Compared to 2D cultured cells, cell viability decreased over the course of 7 days. A higher concentration of chitosan in their PVA ink resulted in a higher cell viability of up to 90.7%.[33] Additionally, Sorkio et al. also used hASCs, as well as human embryonic stem cell-derived limbal epithelial stem cells (hESC-LESCs). Using a commercial assay kit, they tested cell viability on days 3 and 7 and observed high viability with few dead cells; however, the results were not quantified.[45] Kim et al. also used a commercial assay kit to visualize live and dead mesenchymal stem cells after 1 day.[31] They claimed that they did not observe any dead cells. Mörö et al. also used a commercial live/dead viability/cytotoxicity kit and observed high viability of over 95% on day 1 and day 7. With a PrestoBlue™ assay, they further confirmed their high cell viability.[36] Moreover, Kong et al. examined the cell viability within their GelMA hydrogel on day 3 and observed high cell viability.[54] The cell viability was not assessed on their printed scaffold; thus, a possible impairment by the scaffold could not be determined. Zhang et al. analyzed live/dead stained images of human corneal endothelial cells. They concluded that the viability of the cells exceeded 80%.[22] Kim et al. bioprinted human corneal endothelial cells (HCEnCs) onto an amniotic membrane.[30] Before bioprinting, the cells were infected with the ribonuclease (RNase) 5 vector to overexpress RNase, thus leading to enhanced cell proliferation and survival. They compared RNase 5 vector-transfected HCEnCs with HCEnCs and demonstrated that the transfected HCEnCs had a higher population and the typical hexagonal shape of corneal endothelial cells. Thus, Kim et al. demonstrated the advantage of overexpression of RNase 5.

Light transmission

Light transmission and corresponding transparency is one of the fundamental criteria for a functional cornea.[99] Transmission changes will depend on wavelength. In the range of 300–600 nm, a strong increase in transmission can be observed.[106–108] In low wavelength ranges, there is either no transmission or little transmission. This is due to the chromophores of the cornea, which absorb ultraviolet light in the range of 200–295 nm.[109] According to Beems and van Best, transmission in human corneas can reach up to 94%.[107] Similar results were published by Boettner and Wolter. Specifically, they stated that transmission from

500 to 1300 nm is more than 90%.[108] Therefore, for the evaluation of artificial corneas, choosing a broad spectrum from 300 to 780 nm is recommended.

Although Wu et al. stated that their bioprinted cornea is "good" and "clearly visible," in terms of optical transparency, the measurement of light transmittance at 630 nm was only 62.2 ± 8.4%. Therefore, their bioprinted cornea has insufficient transmission and requires further improvement in optical transparency.[29] Zhang et al. measured their bioink with a spectrophotometer at wavelengths of 300–700 nm and found 85%–94% in the visible light spectrum. In the ultraviolet range, the printed construct exhibited low transmittance. The results of Zhang et al. are similar to the values in the aforementioned literature, thus making their bioprinted construct a viable option in terms of light transmission.[22] Similar results were also achieved by Mahdavi et al. for wavelengths of 450–600 nm, the light transmittance was 80%–94%. Additionally, at higher wavelengths, the transmittance was greater than 95%.[19] At all visible wavelengths, Gibney et al. demonstrated an average light transmission of 87.5 ± 6%; thus, their recombinant collagen bioink is suitable for light transmission for corneal bioprinting.[43] Mörö et al. demonstrated a light transmission of only 71.9 ± 1.3% at 400 nm but an increase of up to 94.1 ± 1.5% at 700 nm.[36] Moreover, Ulag et al. measured light transmission between wavelengths of 400 and 800 nm. However, they showed only a "moderate transmittance" of less than 61%. Furthermore, with the addition of chitosan, the light transmission ratio decreased. Therefore, their proposed bioink is not suitable for the bioprinting of transparent corneas.[33] The same wavelength was also used by He et al. to measure light transmission. At 600 nm, their favored bioink exhibited light transmission of 82.5%. However, they demonstrated an increase in light transmission to approximately 90%.[24] Kim et al. and Duarte Campos et al. evaluated their bioprinted construct in terms of optical transparency to native human corneas and rabbit corneas, respectively.[31,42] Both corneas exhibited similar results compared to their control corneas, thus demonstrating high transparency. Additionally, Kutlehria et al. used the method described by Kim et al.[31] to measure light transmission. Briefly, the bioink was melted and poured into the wells of a 48 well plate up to a certain height. Subsequently, light absorption in the wavelength range of 300–700 nm was measured with a microplate reader. The light transmission values were then calculated from the light absorption values. The results of Kutlehria et al. ranged from 75% to 90% depending on the wavelength.[20] Another study by Kong et al. measured light transmission over a period of 28 days. They showed a slight increase in light transmission over time. However, the light transmittance was only 74.7 ± 1.45% at the 500 nm wavelength on day 0. Nevertheless, Kong et al. transplanted their corneal graft into rats and showed high transparency in vivo.[54] Similar to Kong et al., Kilic Bektas and Hasirci evaluated the transparency of the hydrogels over a 3-week time period. They also demonstrated an increase in light transmittance over time from 75% on day 1 to 83%.[34] An overview and comparison of each printed corneal model can be seen in Figure 4.

Biomechanical properties

In all tissues, biomechanical properties play a crucial role in maintaining structure. In particular, the cornea has certain biomechanical properties; for example, the cornea must be robust enough to withstand intraocular pressure. However, at the same time, the cornea must be soft enough to bend in an aspheric dome.[110] The biomechanical properties in vivo depend on many factors. First, components of the extracellular matrix, such as glycosaminoglycans and proteoglycans, influence the mechanical stability of the cornea, as they affect the diameter of the collagen fibrils, the spacing of the fibrils, and the lamellar cohesion properties.[111] Second, hydration impacts the elastic modulus of the cornea. Specifically, hydration decreases the corneal thickness, which results in a decrease in the elastic modulus.[112] Third, each layer of the cornea has a different influence on stiffness. The stroma is the largest contributor to stiffness, as it not only makes up the largest part of the cornea but also contains a large amount of dense collagen fibrils.[113] The contribution of the epithelium to stiffness is lower than that of the stroma; therefore, Elsheikh et al. suggested that its role in the overall mechanical properties could be neglected in simulations.[114]

The mechanical properties of the cornea can be described as viscoelastic properties. From the noncovalent rearrangements of the ECM, such as from water diffusion and electrostatic interactions between glycosaminoglycans and collagen, the viscosity can be determined, which is dynamic and time dependent. Elasticity can be derived from the tensile properties of the collagen microstructure. The action of mechanical stress on collagen fibers leads to elastic deformation. At a certain threshold of mechanical stress, the range of elastic deformation is exceeded, and irreversible plastic deformation occurs. An even higher mechanical stress results in corneal fracture. Moreover, Young's modulus or elastic modulus is one parameter that can be determined to describe elastic deformation. In a stress–strain diagram, it is the slope of the linear portion that represents this factor. Stiffer constructs have a higher Young's modulus.[110] Probably due to different test conditions and methods of the performed in vitro studies, the Young's modulus of the cornea ranges from 0.1 to 57 MPa.[115] A more recent study calculated a mean equilibrium Young's modulus of approximately 0.04 MPa.[116] This wide range makes it difficult to effectively evaluate and compare the results of bioprinted cornea models. An improved evaluation would include an ex vivo cornea using the same method as the bioprinted cornea models. In

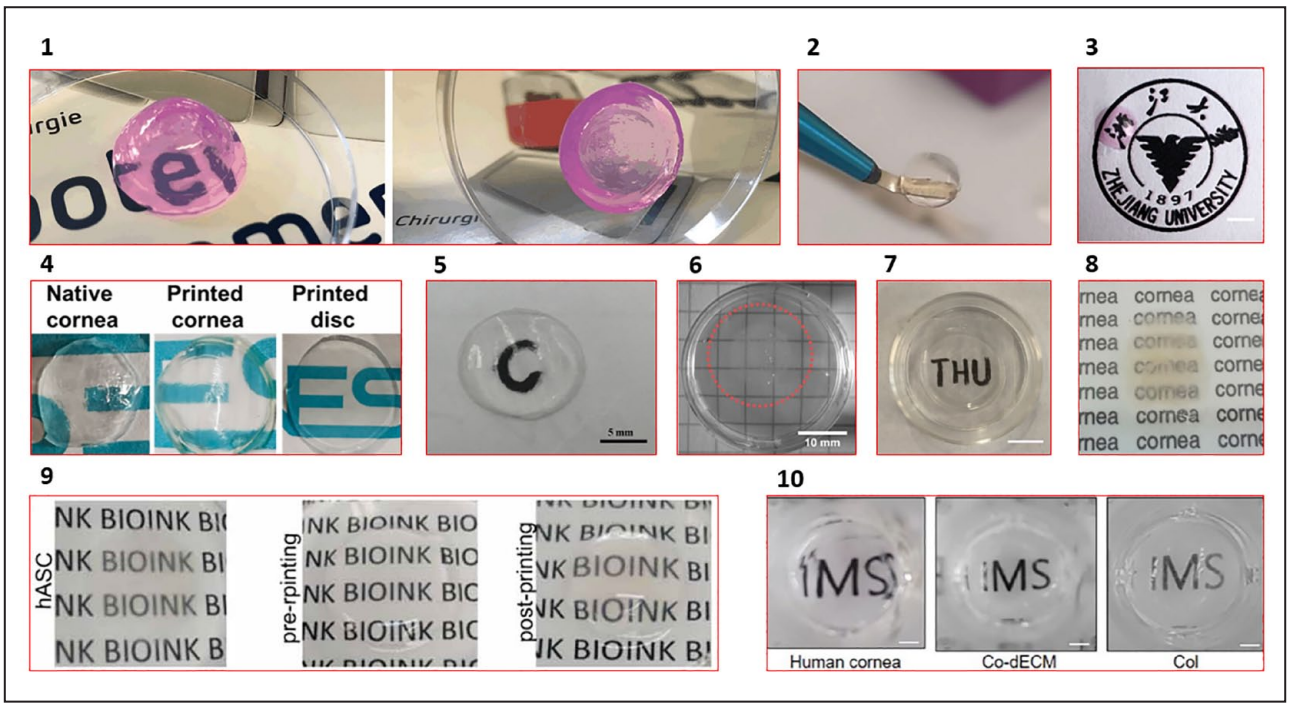

Figure 4. Transparency of different bioprinted corneas. (1) Collagen and agarose with food coloring printed cornea by Duarte Campos et al.[42] (2) A swollen sample of printed collagen on a corneal scalpel by Gibney et al.[43] (3) Alginate and gelatin with food coloring printed cornea by Zhang et al.[14] (4) Comparison of native cornea to printed cornea and printed disc by He et al.[24] (5) Alginate with gelatin and collagen printed cornea by Kutlehria et al.[20] (6) Alginate and ColMA printed corneas by Isaacson et al.[26] (7) Comparison of bioprinted corneas with different differentiation methods of hASCs by Mörö et al.[36] (8) A corneal model consisting of two bioink formulated printed corneas by Sorkio et al.[45] (9) GelMA printed corneas by Kong et al.[54] (10) Comparison of human cornea with printed dECM cornea and collagen as control by Kim et al.[31]

addition to Young's modulus, the tensile strength, which is the maximum stress before breakage, is often determined. An average tensile strength of approximately 3.8 MPa was obtained for the human cornea.[117]

Zhang et al. used a stress–strain measurement with uniaxial loading to determine the tensile strength and the elastic modulus. By using different concentrations of sodium alginate in their bioink, they observed the highest Young's modulus of 0.2 MPa at an alginate concentration of 0.04 g/mL. For the same alginate concentration bioink, a tensile strength of approximately 0.22 MPa was determined. However, Zhang et al. did not use any control for their evaluation.[22] The results of Young's modulus are difficult to evaluate due to the wide range of values in the literature and the lack of a control cornea by Zhang et al. However, 0.2 MPa is located at the low end of Young's modulus of corneas in the literature. Even more notable is the very low tensile strength of approximately 0.22 MPa, which is more than 17 times lower than that of human corneas. These results from Zhang et al. demonstrate questionable mechanical properties of their bioprinted construct. A higher tensile strength, as well as a higher Young's modulus, is crucial to resist intraocular pressure in the eye. Duarte Campos et al. measured a Young's modulus of 0.0181 ± 0.0035 MPa.[42] These results indicate that their bioink is not suitable for mechanical stress. Furthermore, Duarte Campos et al. did not compare their results with a control cornea but only with values from the literature. A similar value of 0.02 MPa was obtained by Kilic Bektas and Hasirci.[34] Specifically, the Young's modulus of their bioprinted construct increased from 0.01 to 0.02 MPa over the course of 21 days. This possibility demonstrates that the HCKs are active and increase biomechanical properties with time. However, they also did not compare their results with a control cornea. Therefore, the results obtained by both groups are questionable because the range of literature values is very wide; therefore, their test methods and results can only be compared with a control. In addition, both sets of results are at the lower end of the range compared to the wide range of literature values. Young's modulus was also measured by Kong et al. They compared their constructs with different pore sizes with the native cornea. Their preferred construct had a Young's modulus of 0.12 ± 0.01 MPa, whereas the native cornea had a Young's modulus of 0.09 ± 0.01 MPA in the same test. Furthermore, Kong et al. examined the tensile strength

of their constructs. The same previously preferred construct achieved a tensile strength of 3.47 ± 0.43 MPa, which is close to the native cornea strength of 3.8 MPa.[54] In conclusion, Kong et al. demonstrated a feasible corneal construct in terms of mechanical properties. Moreover, Ulag et al. achieved a higher tensile strength than that of native corneas, with tensile strengths of up to 40.28 MPa being obtained. With the addition of chitosan to the polyvinylalcohol bioink, the tensile strength decreased to 8.94 MPa with 5% chitosan.[33] These values represent more than double the tensile strength of native corneas. To further evaluate its construction and mechanical properties, the use of Young's modulus is essential. Zhong et al. determined Young's modulus by using a micromechanical testing machine with a 10% strain and a strain rate of 2 µm/s. As GelMA and HAGM, these bioinks depend on UV crosslinking and crosslinking time. With increasing exposure time, Young's modulus also increased up to 0.015 MPa.[23] Gibney et al. measured Young's modulus by using nanoindentation, thus resulting in a Young's modulus of 0.506 ± 0.173 MPa compared to the 0.281 ± 0.214 MPa Young's modulus value of the human anterior cornea stroma. They also stated that further testing is needed to fully evaluate the biomechanical properties of their proposed model.[43] He et al. measured tensile strength and Young's modulus with a microtester, resulting in values of 0.0822 and 0.1007 MPa, respectively. They also measured a native cornea, which provided values of 0.1218 and 0.1153 MPa for tensile strength and Young's modulus, respectively. Thus, their printed corneal constructs had approximately 33% and 13% lower tensile strength and Young's modulus, respectively, than the native cornea.[24] Only Young's modulus was measured by Mörö et al. via a hybrid rheometer, thus resulting in a Young's modulus of 0.0103 MPa.[36] They did not measure a native cornea for comparison. This indicates that their construct is at the lower end of the literature values and is also the lowest of all measured Young's moduli of printed corneal models.

3D modeling

Besides the biomechanical properties to withstand intraocular pressure, the shape of the cornea to be transplanted is also essential. For example, Duarte Campos et al., Mahdavi et al. as well as Kutlehria et al. created their corneal models based on literature data using CAD software.[19,20,42] Another option is to obtain data from patients and use this data to create corneal models. This was done by Isaacson et al. who used a rotating Scheimflug camera to create the model.[26] A similar method was implemented by Zhang et al., who used a commercial scanning instrument and mathematical modeling to create the corneal model.[22] Due to the curvature of the corneal model, a support structure is often needed. For example, Kutlehria et al. printed a support scaffold with an FDM printer using PLA in a high-throughput method.[20] Ulag et al. used an aluminum mold based on a corneal model. In this model the corneal scaffold was printed.[33] Another option is to use a sacrificial support scaffold; this was done by Mahdavi et al., who used sacrificial gelatin to support the curvature of the cornea.[19] To avoid the use of support scaffolds, DLP printing can be a promising method. Nevertheless, Kim et al. further improved their crosslinking after extrusion printing by using a ruthenium/sodium persulfate crosslinker in combination with light to achieve a rapid crosslinking to create more complex geometric constructs such as the cornea.[118]

Expression of specific proteins and genes

A total of 3250 unique proteins have been identified in the cornea. Different proteins have been identified according to the layer; however, 609 unique proteins have been found in the epithelium, stroma, and endothelium. Although the stroma constitutes the largest part of the cornea, the highest number of unique proteins was identified in the epithelium. At 47%, keratins constitute the highest proportion of the proteins of the epithelium.[101] Cytokeratins 3 and 12 play an important role in maintaining the integrity of the corneal epithelium.[119] The corneal stroma contains more than 1600 unique proteins.[101] The proteins can be classified into gel-like organic materials and filament networks. The category of gel-like organic material includes proteoglycans, glycoproteins, and enzymes, as well as binding and serum proteins.[120] Moreover, proteoglycans such as decorin, lumican, and keratocan play a pivotal role in maintaining corneal transparency by regulating the structure of lamellar and collagen fibrils by maintaining collagen fibers at a defined distance.[111,121,122] Furthermore, a mutation in the decorin gene, which results in truncated decorin, and accumulation are associated with congenital stromal corneal dystrophy.[123,124] Fibronectin and laminin, together with elastin, keratin, vimentin, and collagens, can be classified in the filament network.[120] Moreover, type I and type VI collagen are the most common collagens in the stroma.[119] However, when an injury occurs, keratocytes differentiate into fibroblasts or myofibroblasts. Fibroblasts and myofibroblasts express the specific protein marker alpha-smooth muscle actin (α-SMA), which contributes to corneal opacity.[125] Vimentin, which is an intermediate filament, can also be found in fibroblasts.[119,126] Therefore, in artificial bioprinted corneal stroma, the expression of α-SMA and vimentin is not desired.

Kim et al., Duarte Campos et al., and Kilic Bektas and Hasirci tested for α-SMA.[32,34,42] They did not observe expression of α-SMA. Kim et al. tested not only α-SMA but also type I collagen and keratocan, as well as the gene expression of keratocyte-specific genes such as KERA and ALDH and the gene ACTA2, which are characteristic markers of myofibroblasts. Compared to nonprinted samples, their model exhibited a higher expression of keratocan, a more than 1500-fold change for KERA, a more

than 10-fold change for ALDH, and a similarly low gene expression of ACTA2. Furthermore, they showed an increase in type I collagen over the span of 28 days in both nonprinted and printed samples.[32] Moreover, Duarte Campos et al. investigated the expression of keratocan and lumican and demonstrated positive expression for both markers compared to native human corneal stromal tissue.[42] Kilic Bektas and Hasirci examined the expression of type I and type VI collagen, as well as decorin, on bioprinted constructs with different layer heights compared to a nonprinted slab. They were able to detect only low levels at the core, thus leading to the assumption that cells were only able to express higher levels of collagen and decorin at the edges of the line. Moreover, compared to the nonprinted slab, no correlated changes were observed.[34] Wu et al. examined the protein expression of cytokeratin 3 in their printed scaffolds with HCECs in a gelatin alginate collagen matrix. They demonstrated an increase in cytokeratin 3 from day 1 to day 5. Wu et al. claimed that this increase demonstrates that cells can normally proliferate and "strongly express proteins.". However, no comparison was made with a 2D model or a native cornea. However, they have shown that faster degradation via the addition of sodium citrate to breakdown alginate results in an overall increase in proliferation and cytokeratin 3 expression.[29] Similar to Wu et al., Sorkio et al. examined the protein expression of cytokeratin 3. Furthermore, they examined the protein expression of cytokeratin 15, Ki67, p63α, p40, VWF, and type I collagen. Due to the fact that Sorkio et al. used two different stem cells human embryonic stem cell derived limbal epithelial stem cells (hESC-LESCs) and human adipose tissue-derived stem cells (hASCs), which differentiate into epithelial cells and stromal-mimicking cells, respectively, different markers were examined for each cell type. For the differentiation of hESC-LESCs into epithelial cells, the markers of cytokeratin 3 and 15, which are specific proteins of corneal epithelial cells, Ki67, a proliferation marker, and p63α and p40, markers for the corneal progenitor, were studied. With the exception of Ki67, which was only detectable in a few cells, all markers exhibited high expression. When hASCs were differentiated into stromal-implicating cells, the expression of type I collagen and VWF showed positive labeling. However, it should be noted that differentiation into corneal epithelial and stromal cells needs to be further investigated to be fully understood.[45] Moreover, Kutlehria et al. decided to detect fibronectin and f-actin, both of which can be found outside of the human cornea. Therefore, although these proteins are not specific to the cornea, fibronectin and f-actin are important for the alignment and high order of the corneal stromal extracellular matrix.[127,128] Kutlehria et al. demonstrated the expression of fibronectin and f-actin.[20] Additionally, Kong et al. used limbal stromal stem cells (LSSCs) differentiated into keratocytes. To further determine the typical phenotype of quiescent keratocytes, they examined the specific marker protein ALDH3A1 and type VI collagen. Furthermore, Kong et al. evaluated the gene expression of ALDH3A1, keratocan, and aquaporin 1 via qPCR. To exclude the possibility that limbal stem cells differentiated into fibroblasts, Kong et al. further examined specific fibroblast markers, such as the protein vimentin, and the gene expression of thymocyte antigen 1. The results were evaluated and compared to those of 2D cultured models with and without serum in the medium. The addition of serum to the medium favored differentiation into fibroblasts, as the expression of thymocyte antigen 1 was higher than in nonserum media. Moreover, the printed construct had higher gene expression of ALDH3A1, keratocan, and aquaporin 1 than the 2D cultured model. The protein labeling of vimentin and ALDH3A1 in the printed construct was aligned compared to the randomly labeled proteins in the 2D cultured model. However, the expression of vimentin was minimal compared to the 2D cultured model.[54] As Zhong et al. aimed to demonstrate the effect of the ECM with two different bioinks on rabbit and human limbal stem cells (rbLSCs and hLSCs, respectively) in relation to the active and quiescent statuses, they examined various protein markers, as well as gene expression, in comparison with a 2D model. Ki67 and △NP63, which are both proliferation markers, and PAX6, which is an LSC lineage marker, were investigated after 2 days of culture. Zhong et al. showed that the expression of KI67 was higher in GelMA scaffolds. Moreover, △NP63 and PAX6 were equally expressed in each scaffold. They also demonstrated that the specific genes of the quiescent state, such as CD200 and $P27^{KIPI}$, were upregulated in the HAGM print. Furthermore, other markers, such as PAX6, BMI1, VANGL1, and WNT5A, were upregulated in the HAGM group but downregulated in the GelMA print group. In the GelMA group, P63 was upregulated, whereas other markers, such as KRT3, VANGL1, and WNT5A, were downregulated. In conclusion, they demonstrated quiescent properties in the HAGM scaffold.[23] Mahdavi et al. investigated the protein expression of type I collagen and lumican, as well as the gene expression of type I collagen, lumican, and keratan sulfate. After 14 days, they demonstrated an increase in all markers in 3D bioprinted constructs compared to cultured 2D models.[19] After printing, Mörö et al. demonstrated positive expression of the proliferation marker Ki67 in hASC-CSK. Furthermore, positive expression of lumican was observed in hASC-CSK. To detect cell–cell interactions in printed structures, staining was performed against connexin 43 was conducted, thus resulting in positive expression. In hASC-CSK, vimentin expression was low.[36] Furthermore, in corneal keratocytes, low levels of vimentin were considered normal.[126] The gene expression of vimentin and lumican increased compared to that in undifferentiated hASCs,

but lower than that in hCSKs. Moreover, positive expression of ALDH3A1, collagen V, and keratocan was detected.[36]

Swelling and degradation

When natural corneas, especially the stroma, swell, they become cloudy due to higher light scattering, and vision becomes impaired.[129] Furthermore, swollen corneas are thicker, thus increasing the porosity of collagen lamellae and leading to an increase in permeability.[112] This is important both for artificial corneas, as the cornea is the first biological barrier, as well as for in vitro corneal models; for example, drug permeability is a key element for drug testing. Therefore, for cornea models, it is important that swelling is limited to a certain level, which occurs in native corneas. Swelling can be calculated as

$$S_w = \left(m_{wet} - m_{dry}\right) / m_{dry}$$

where m_{wet} and m_{dry} are the wet and dry weights of the cornea, respectively. It is important to examine how long and in what type of medium the swelling is examined. Additionally, care must be taken to choose a medium that has a saline concentration to the in vivo environment. Zhang et al. evaluated the swelling of their bioprinted corneal models for 24 h in distilled water, which resulted in an average increase of 15%.[22] Distilled water most likely leads to higher levels of swelling due to diffusion. This environment also leads to a decrease in cell viability. Therefore, their results are questionable with respect to the use of distilled water as their medium of choice. Moreover, Ulag et al. investigated the swelling of their bioprinted cornea models in PBS for 1 week. All of their cornea models exhibited a considerable increase in swelling between 300% and 560%. They also showed that the increase was greatest within the first 24 h. After the first day, a slight decrease was noted over the course of 1 week.[33] Additionally, Kong et al. used the same method to compare the swelling of their bioprinted corneal models with native corneas. The native cornea exhibited a mass swelling ratio of 14.5 ± 0.59 compared to a mass swelling ratio of 13.9 ± 0.49 of its preferred bioprinted model. For the mass swelling ratio, the samples were incubated in PBS at 37°C for 24 h. The mass swelling ratio was calculated as the division of the wet weight by the dry weight. Their results were similar to the native cornea; thus, in terms of swelling, their bioprinted construct showed promising results.[54] Gibney et al. incubated their samples in PBS at 4°C for 24 h before measuring the swelling ratio. They observed a swelling ratio of $6.8 \pm 1.6\%$. Moreover, they estimated some swelling, since they assumed that their final swollen construct would be 330 nm thick.[43] Bioprinted models should degrade over time so that the cells can express the ECM in a timely manner, thus leading to tissue regeneration and repair in vivo. Therefore, the absolute weight must remain the same for a certain period of time because the matrix is dismantled and built up at the same speed. Therefore, it is essential that bioinks are biodegradable. Cells express matrix metalloproteases, such as collagenase and gelatinase, which help to degrade bioink. Degradation studies have been conducted by four groups. Sorkio et al. demonstrated degradation with a loss of half of its original mass over the course of 8 days.[45] This suggests that the degradation rate was very high. Additionally, slower degradation presumably exhibits less loss over time, which likely has a positive effect on biomechanical stability over time. Sorkio et al. did not evaluate biomechanical properties; therefore, this thesis could not be supported by their study. Decreased loss was achieved by Kilic Bektas and Hasirci.[34] They observed only a loss of 8% after 3 weeks. Furthermore, an increase in Young's modulus was observed during the same time period. This suggests that the degradation loss of 8% can be neglected because the biomechanical property of the Young's modulus increased. However, the tensile strength was not measured. Mörö et al. evaluated both swelling and degradation. They observed a slight increase in swelling in the first 3 h, followed by a degradation of approximately 20% on day 3, which stagnated until day 14.[36] Similar to Mörö et al., He et al. also evaluated swelling and degradation. For swelling, they immersed the hydrogel in PBS at 37°C and measured the swelling ratio over 4 weeks. After several days, swelling increased to approximately 100% and continued until day 28. For degradation, they also incubated their hydrogel in PBS with collagenase at 37°C for 4 weeks. In the first week, faster degradation was observed, which slowed down until less than 50% residual weight was obtained at the end of the 4-week time period.[24]

In vivo study

To our knowledge and to date, no bioprinted models have been transplanted into humans. Kim et al. transplanted their bioprinted corneal model into ten New Zealand white rabbits. They transplanted 5 printed models and 5 nonprinted control models. The transplanted printed model of Kim et al. was more transparent than the nonprinted counterpart.[32] In another study, which was also conducted by Kim et al., type I collagen gel was compared to Co-dECM in mice and rabbits. In mice, the immune response to each gel was individually examined, thus showing that the Co-dECM gel resulted in fewer immune cells than the type I collagen gel. Furthermore, when transplanted into rabbit corneal pockets, there was higher expression of KERA in the Co-dECM gel group than in the type I collagen gel group. The cell density was similar in both groups.[31]

Park et al. used decellularized stromal ECM with differentiated keratocytes from human turbinate-derived

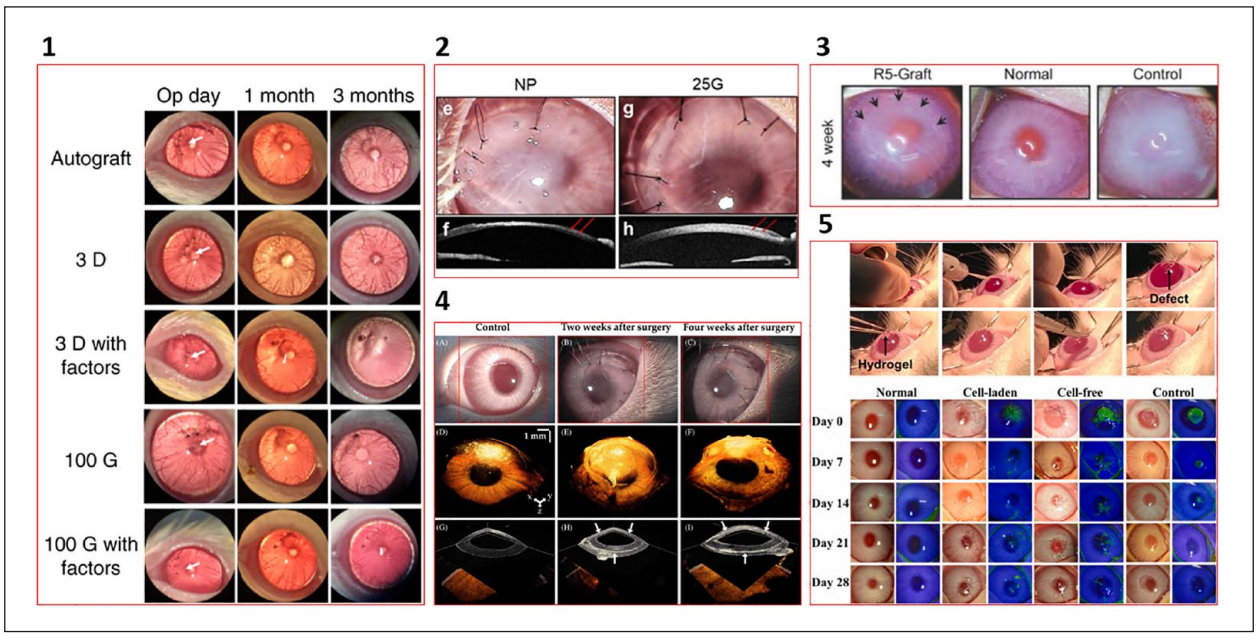

Figure 5. In vivo studies of bioprinted corneas. (1) Comparison of printed cornea (100 g) with nonprinted cornea (3D), each with and without factors, and autograft as control over the course of 3 months, conducted by Kong et al.[54] (2) Comparison of nonprinted cornea and printed cornea (25 G) conducted by Kim et al.[31] (3) Comparison of R5 HCEnC AM graft with normal cornea and control cornea without Descemets membrane over the course of 4 weeks conducted by Kim et al.[30] (4) Slit-lamp microscopic images of control and printed corneas 2 and 4 weeks after surgery complemented by 3D-rendered images and optical coherence tomography images, conducted by Park et al.[35] (5) Surgical procedure of keratoplasty, as well as comparison of normal cornea, cell-laden, cell-free, and control cornea, over the course of 4 weeks. The green area shows the corneal epithelial defect, conducted by He et al.[24]

mesenchymal stem cells (hTMCS) printed and cultured for 4 weeks before implantation in five white male rabbits. The bioprinted constructs were not previously evaluated in regards to cell viability, biomechanical properties, and light transmission. They monitored the transplanted corneal models by using swept-source optical coherence tomography. Via this method, Park et al. assessed the thickness of the transplanted cornea. A slight increase was observed in the first 2 weeks, which was presumably due to edema from surgery. Subsequently, a decrease was observed in the following weeks. After 4 weeks, the transplants were extracted and stained with hematoxylin and eosin to evaluate the immune responses. Few inflammatory cells were solely observed in the bioprinted corneas. Nevertheless, no T cells were identified.[35]

Kong et al. demonstrated the viability of their printed model with intrastromal keratoplasty in rats over a 12-week period. They compared their printed models with the nonprinted model, each with and without factors. As a positive control, they transplanted autografts into 6 rats. After the 3-month study, they concluded that the printed model with factors resulted in improved keratocyte morphology and a better chemical environment, which favored stromal tissue regeneration.[54]

Kim et al. transplanted RNase 5 vector-transfected (RN5) HCEnC AM grafts, HCEnC AM grafts, and acellular bovine AMs after descemetorhexis in a procedure similar to Descemet stripping with automated endothelial keratoplasty (DSEK) in rabbits. In addition, a cell suspension of HCEnC was injected into the anterior chamber. In all cases, both the pupillary margin and the anterior chamber structures were obscured. However, microscopic observations demonstrated clearance of the HCEnC AM graft and the R5 HCEnC AM graft over the course of 4 weeks. In addition, the RN5 HCEnC AM graft was clearer than the HCEnC AM graft and more similar to a normal clear cornea. They also demonstrated that the RN5 HCEnC AM and HCEnC AM grafts were attached to the corneal stroma. Furthermore, the protein expression of specific corneal endothelial markers, such as Na^+-K^+-ATPase, zonula occludens (ZO-1), CD44, and CD166, was examined. Kim et al. demonstrated that specific marker expression was higher in RN5 HCEnC AM grafts than in HCEnC AM grafts. However, in all transplants, corneal edema could be detected, since the corneal central thickness was greater than 1000 µm. A significant decrease in the corneal central thickness could only be measured after 2 weeks in the grafts with HCEnC.[30]

He et al. used seven white rabbits and transplanted a bilayer of their bioprinted PEGDA-GelMA hydrogel with rCECs and rASCs that mimicked the epithelium and stroma, respectively. Before transplantation, the bioprinted bilayer was cultivated for 4 days. They also examined seven other rabbits with cell-free hydrogels, as well as seven rabbits as controls. As a control, only a corneal defect was created. These researchers were able to demonstrate an improvement in corneal healing with their cell-laden bilayer construct. The cell-laden bilayer construct healed faster than the control and remained transparent for a period of 28 days. Furthermore, improved regeneration was demonstrated by higher Col I and CK3 staining in the bioprinted constructs. In addition, the high expression of lumican and low expression of αSMA indicated that the rASCs differentiated into keratocytes rather than into myofibroblasts. The typical gene expression of keratocyte specific markers, such as KERA, ALDH3A1, and AQP1, was also similar to that of native corneas.[24] An overview and comparison of each transplanted bioprinted corneal model can be seen in Figure 5.

Outlooks and future perspectives

The advantages of bioprinting compared to conventional tissue engineering methods include high throughput, spatial control for high precision, and rapid production of multilayer constructs. It is also possible to produce patient-specific corneas because the 3D model and the parameters of a printer can be easily adjusted. In general, a major limitation of bioprinting is the vascularization of the bioprinted constructs. However, the cornea is a relatively small avascular structure, thus making it an attractive model for bioprinting. Nevertheless, there are still limitations and challenges that need to be addressed in the future of cornea bioprinting. First, the cornea has a specific geometry with a unique curvature. Second, it is difficult to formulate a bioink that is not only transparent but also has biomechanical properties such as elastic modulus and tensile strength, thus allowing the artificial cornea to be transplanted and sutured. Third, corneal cells such as epithelial cells, keratocytes, and endothelial cells express a variety of specific proteins. More research is needed to fully understand the effects of bioprinting on protein expression.

Stem cells have the potential to be used and differentiated into any of the aforementioned cell types. However, they are associated with higher costs, less availability, and more ethical problems; in addition, there is a greater need for research on growth factors and differentiation than for primary cells.[130] To our knowledge, a medium and composition of growth factors more suitable for the bioprinting of limbal stem cells has not yet been developed. Human corneal epithelial cells form a characteristic layer of basal cells and flat cells on the top surface. To our knowledge, this differentiation and migration of basal epithelial cells has not yet been demonstrated. Human corneal keratocytes have a characteristic dendritic shape; moreover, to maintain this shape, bioinks and print parameters, such as extrusion force and printing speed, must be controlled. Furthermore, as one of the first protective barriers to the eye, the cornea has a large number of immune cells.[101] The characteristic composition of the immune system in bioprinted models has not yet been investigated, although this scenario is crucial for transplantation and acceptance in vivo. To further evaluate bioprinted cornea models, more in vivo tests need to be performed. This is to ensure that the model is biocompatible and biodegradable and that it produces little to no immune response while maintaining biomechanical integrity and transparency. Future clinical trials should be conducted to evaluate this possibility. Currently, most bioprinted corneal models implement only one type of cell. The implementation of all three major cell types, epithelial cells, keratocytes, and endothelial cells, is still pending. In addition to implementing more than one cell type, it may be an improvement to implement a combination of different technologies, as each cell layer has different expectations for printability. This will also lead to the use of two or more different bioinks, which are more similar to the native environment, as each layer is composed of different biomaterials.

To address the issues mentioned above, novel printing technologies, such as 4D bioprinting and cell electrowriting, can provide a solution. In 4D bioprinting, the printed construct changes over time, such as based on its geometry. To trigger these events, adaptation to the environment or the addition of chemical factors is needed. This 4D bioprinting can lead to a more dynamic model.[131] Moreover, cell electrowriting combines the use of electrowriting with cells. This method allows for higher resolution and more accurate layering of collagen fibers, which corresponds to the natural arrangement of collagen fibers in the corneal stroma.[132] Novel bioinks and biomaterials that can improve mechanical integrity are also needed. Novel materials should be more reproducible, have low environmental impact, and be harmless to animals. This has already been proposed as "clean bioprinting."[133] This scenario will also apply to corneal bioprinting.

As bioprinting is fairly new, and no commercialized product has been developed to date, no regulations currently affect bioprinting, as it is "in-between existing categories of living and non-living materials"; therefore, it is proposed as representing "bio-objects."[134] Nevertheless, it is likely that for clinical approval, the bioprinted cornea must possess data on preclinical and clinical studies conducted under good clinical practice, whereas production is performed under good manufacturing practices (GMP), similar to studies that have already been conducted with tissue-engineered corneas.[135,136] Currently, all of the

research in terms of cornea bioprinting is still far from clinical testing. All of these new upcoming technologies may raise further questions, especially regarding ethical complications. First, the type and origin of cells must be clarified before human use can be considered. Cells could be stem cells, such as mesenchymal, induced pluripotent, or limbal stem cells, as well as primary cells. For all cells, the origin is important because safety must be considered. The use of stem cells for tissue engineering is still considered a risk, as studies have demonstrated possible cancer-increasing risks, contamination with microorganisms or viruses, and immune response.[137] An alternative to this possibility can be cells obtained from the patient. This may reduce the risk of further complications and reduce the use of immunosuppressants. Furthermore, stem cells are currently associated with higher costs, thus leading to global inequalities, as their availability is limited to higher earning countries and people.[138] Second, variability can occur, whether it is related to donations, in vitro cultivation, or in vivo transplantations.[137] However, the cornea is not directly connected to blood or lymph vessels. This reduces the risk of implanted cells migrating to other parts of the body, which may increase the risk of adverse effects. As bioprinting improves, it must be considered that it is possible to create enhanced corneas with improved vision. This raises further ethical questions, such as the limits of experimentation and who is entitled to a transplant.

Conclusions

Corneal bioprinting has a high potential and is also feasible and viable. This method can improve the global situation of a shortage of donor corneas in the future. In addition, improved 3D bioprinted models can also advance research in in vitro diagnostics for drug testing. Research has shown that bioprinting is capable of achieving the goals of high cell viability, light transmission, and biomechanical properties on its own. Nevertheless, there are still limitations to achieving excellent results in all properties, such as sufficient biomechanical properties in combination with high light transmission and cell viability. Furthermore, more research is needed in terms of in vivo evaluation, as in vitro and in vivo studies still demonstrate considerable differences. In the near future, these obstacles will be overcome, and bioprinting will establish itself as an advanced method compared to the current state of tissue engineering.

Availability of data and materials

All data or related information supporting the conclusions of the review is included in the article.

Declaration of conflicting interests

The author(s) declared no potential conflicts of interest with respect to the research, authorship, and/or publication of this article.

Funding

The author(s) disclosed receipt of the following financial support for the research, authorship, and/or publication of this article: The APC was funded by Open Access Publication Funds of Technische Universität Braunschweig.

ORCID iD

Stephan Reichl https://orcid.org/0000-0001-8344-9070

References

1. Flaxman SR, Bourne RRA, Resnikoff S, et al. Global causes of blindness and distance vision impairment 1990-2020: a systematic review and meta-analysis. *Lancet Glob Health* 2017; 5: e1221–e1234.
2. Bailey R and Lietman T. The SAFE strategy for the elimination of trachoma by 2020: will it work? *Bull World Health Organ* 2001; 79: 233–236.
3. Gambhir M, Basáñez M-G, Turner F, et al. Trachoma: transmission, infection, and control. *Lancet Infect Dis* 2007; 7: 420–427.
4. Oliva MS, Schottman T and Gulati M. Turning the tide of corneal blindness. *Indian J Ophthalmol* 2012; 60: 423–427.
5. Vajpayee RB, Vanathi M, Tandon R, et al. Keratoplasty for keratomalacia in preschool children. *Br J Ophthalmol* 2003; 87: 538–542.
6. De Miguel MP, Alio JL, Arnalich-Montiel F, et al. Cornea and ocular surface treatment. *Curr Stem Cell Res Ther* 2010; 5: 195–204.
7. Matthaei M, Sandhaeger H, Hermel M, et al. Changing indications in penetrating keratoplasty: a systematic review of 34 years of global reporting. *Transplantation* 2017; 101: 1387–1399.
8. Mathews PM, Lindsley K, Aldave AJ, et al. Etiology of global corneal blindness and current practices of corneal transplantation: a focused review. *Cornea* 2018; 37: 1198–1203.
9. Tan DT, Dart JK, Holland EJ, et al. Corneal transplantation. *Lancet* 2012; 379: 1749–1761.
10. Gain P, Jullienne R, He Z, et al. Global survey of corneal transplantation and eye banking. *JAMA Ophthalmol* 2016; 134: 167–173.
11. Ludwig PE, Huff TJ and Zuniga JM. The potential role of bioengineering and three-dimensional printing in curing global corneal blindness. *J Tissue Eng* 2018; 9: 2041731418769863.
12. Groll J, Boland T, Blunk T, et al. Biofabrication: reappraising the definition of an evolving field. *Biofabrication* 2016; 8: 013001.
13. Guillemot F, Mironov V and Nakamura M. Bioprinting is coming of age: report from the International Conference on Bioprinting and Biofabrication in Bordeaux (3B'09). Biofabrication 2010; 2: 10201.
14. Zhang B, Xue Q, Li J, et al. 3D bioprinting for artificial cornea: challenges and perspectives. *Med Eng Phys* 2019; 71: 68–78.
15. Reichl S. Cell culture models of the human cornea — a comparative evaluation of their usefulness to determine ocular drug absorption in-vitro. *J Pharm Pharmacol* 2010; 60: 299–307.

16. Shiju TM, Carlos de Oliveira R and Wilson SE. 3D in vitro corneal models: a review of current technologies. *Exp Eye Res* 2020; 200: 108213.
17. Sommer AC and Blumenthal EZ. Implementations of 3D printing in ophthalmology. *Histochem Cell Biol* 2019; 257: 1815–1822.
18. Savini A and Savini GG. A short history of 3D printing, a technological revolution just started. In: *2015 ICOHTEC/ IEEE international history of high-technologies and their socio-cultural contexts conference (HISTELCON)*, Tel-Aviv, Israel, 18–19 August 2015, pp.1–8. New York, NY: IEEE.
19. Mahdavi SS, Abdekhodaie MJ, Kumar H, et al. Stereolithography 3D bioprinting method for fabrication of human corneal stroma equivalent. *Ann Biomed Eng* 2020; 48: 1955–1970.
20. Kutlehria S, Dinh TC, Bagde A, et al. High-throughput 3D bioprinting of corneal stromal equivalents. *J Biomed Mater Res Part B Appl Biomater* 2020; 108: 2981–2994.
21. Moroni L, Boland T, Burdick JA, et al. Biofabrication: a guide to technology and terminology. *Trends Biotechnol* 2018; 36: 384–402.
22. Zhang B, Xue Q, Hu HY, et al. Integrated 3D bioprinting-based geometry-control strategy for fabricating corneal substitutes. *J Zhejiang Univ Sci B* 2019; 20: 945–959.
23. Zhong Z, Balayan A, Tian J, et al. Bioprinting of dual ECM scaffolds encapsulating limbal stem/progenitor cells in active and quiescent statuses. *Biofabrication* 2021; 13: 044101.
24. He B, Wang J, Xie M, et al. 3D printed biomimetic epithelium/stroma bilayer hydrogel implant for corneal regeneration. *Bioact Mater* 2022; 17: 234–247.
25. Murphy SV and Atala A. 3D bioprinting of tissues and organs. *Nat Biotechnol* 2014; 32: 773–785.
26. Isaacson A, Swioklo S and Connon CJ. 3D bioprinting of a corneal stroma equivalent. *Exp Eye Res* 2018; 173: 188–193.
27. Seol Y-J, Kang H-W, Lee SJ, et al. Bioprinting technology and its applications. *Eur J Cardiothorac Surg* 2014; 46: 342–348.
28. Yilmaz B, Tahmasebifar A and Baran ET. Bioprinting technologies in tissue engineering. *Adv Biochem Eng Biotechnol* 2020; 171: 279–319.
29. Wu Z, Su X, Xu Y, et al. Bioprinting three-dimensional cell-laden tissue constructs with controllable degradation. *Sci Rep* 2016; 6: 24474.
30. Kim KW, Lee SJ, Park SH, et al. Ex vivo functionality of 3D bioprinted corneal endothelium engineered with ribonuclease 5-overexpressing human corneal endothelial cells. *Adv Healthc Mater* 2018; 7: e1800398.
31. Kim H, Park M-N, Kim J, et al. Characterization of cornea-specific bioink: high transparency, improved in vivo safety. *J Tissue Eng* 2019; 10: 2041731418823382.
32. Kim H, Jang J, Park J, et al. Shear-induced alignment of collagen fibrils using 3D cell printing for corneal stroma tissue engineering. *Biofabrication* 2019; 11: 035017.
33. Ulag S, Ilhan E, Sahin A, et al. 3D printed artificial cornea for corneal stromal transplantation. *Eur Polym J* 2020; 133: 109744.
34. Kilic Bektas C and Hasirci V. Cell loaded 3D bioprinted GelMA hydrogels for corneal stroma engineering. *Biomater Sci* 2019; 8: 438–449.
35. Park J, Lee K-P, Kim H, et al. Biocompatibility evaluation of bioprinted decellularized collagen sheet implanted in vivo cornea using swept-source optical coherence tomography. *J Biophotonics* 2019; 12: e201900098.
36. Mörö A, Samanta S, Honkamäki L, et al. Hyaluronic acid based next generation bioink for 3D bioprinting of human stem cell derived corneal stromal model with innervation. *Biofabrication* 2022; 15: 015020.
37. Kyle S, Jessop ZM, Al-Sabah A, et al. Printability' of candidate biomaterials for extrusion based 3D printing: state-of-the-art. *Adv Healthc Mater* 2017; 6: 1700264.
38. Adhikari J, Roy A, Das A, et al. Effects of processing parameters of 3D bioprinting on the cellular activity of bioinks. *Macromol Biosci* 2021; 21: e2000179.
39. Gudapati H, Dey M and Ozbolat I. A comprehensive review on droplet-based bioprinting: past, present and future. *Biomaterials* 2016; 102: 20–42.
40. Wilson WC Jr and Boland T. Cell and organ printing 1: protein and cell printers. *Anat Rec A Discov Mol Cell Evol Biol* 2003; 272: 491–496.
41. Cui X, Boland T, D'Lima DD, et al. Thermal inkjet printing in tissue engineering and regenerative medicine. *Recent Pat Drug Deliv Formul* 2012; 6: 149–155.
42. Duarte Campos DF, Rohde M, Ross M, et al. Corneal bioprinting utilizing collagen-based bioinks and primary human keratocytes. *J Biomed Mater Res A* 2019; 107: 1945–1953.
43. Gibney R, Patterson J and Ferraris E. High-resolution bioprinting of recombinant human collagen type III. *Polymers* 2021; 13: 2973.
44. Barron JA, Wu P, Ladouceur HD, et al. Biological laser printing: a novel technique for creating heterogeneous 3-dimensional cell patterns. *Biomed Microdevices* 2004; 6: 139–147.
45. Sorkio A, Koch L, Koivusalo L, et al. Human stem cell based corneal tissue mimicking structures using laser-assisted 3D bioprinting and functional bioinks. *Biomaterials* 2018; 171: 57–71.
46. Antoshin AA, Churbanov SN, Minaev NV, et al. LIFT-bioprinting, is it worth it? *Bioprinting* 2019; 15: e00052.
47. Ferris CJ, Gilmore KG, Wallace GG, et al. Biofabrication: an overview of the approaches used for printing of living cells. *Appl Microbiol Biotechnol* 2013; 97: 4243–4258.
48. Leberfinger AN, Dinda S, Wu Y, et al. Bioprinting functional tissues. *Acta Biomater* 2019; 95: 32–49.
49. Dou C, Perez V, Qu J, et al. A state-of-the-art review of laser-assisted bioprinting and its future research trends. *CBEN* 2021; 8: 517–534.
50. Kade JC and Dalton PD. Polymers for melt electrowriting. *Adv Healthc Mater* 2021; 10: e2001232.
51. Kong B and Mi S. Electrospun scaffolds for corneal tissue engineering: a review. *Materials* 2016; 9: 614.
52. Blackstone BN, Gallentine SC and Powell HM. Collagen-based electrospun materials for tissue engineering: a systematic review. *Bioengineering* 2021; 8: 39.

53. Sizeland KH, Hofman KA, Hallett IC, et al. Nanostructure of electrospun collagen: do electrospun collagen fibers form native structures? *Mater* 2018; 3: 90–96.
54. Kong B, Chen Y, Liu R, et al. Fiber reinforced GelMA hydrogel to induce the regeneration of corneal stroma. *Nat Commun* 2020; 11: 1435.
55. Vanaei S, Parizi MS, Vanaei S, et al. An overview on materials and techniques in 3D bioprinting toward biomedical application. *Eng Regen* 2021; 2: 1–18.
56. Li W, Wang M, Ma H, et al. Stereolithography apparatus and digital light processing-based 3D bioprinting for tissue fabrication. *iScience* 2023; 26: 106039.
57. Groll J, Burdick JA, Cho D-W, et al. A definition of bioinks and their distinction from biomaterial inks. *Biofabrication* 2018; 11: 013001.
58. Mancha Sánchez E, Gómez-Blanco JC, López Nieto E, et al. Hydrogels for bioprinting: a systematic review of hydrogels synthesis, bioprinting parameters, and bioprinted structures behavior. *Front Bioeng Biotechnol* 2020; 8: 776.
59. Lee A, Hudson AR, Shiwarski DJ, et al. 3D bioprinting of collagen to rebuild components of the human heart. *Science* 2019; 365: 482–487.
60. Yin J, Yan M, Wang Y, et al. 3D bioprinting of low-concentration cell-laden gelatin methacrylate (GelMA) bioinks with a two-step cross-linking strategy. *ACS Appl Mater Interfaces* 2018; 10: 6849–6857.
61. Duan B, Hockaday LA, Kang KH, et al. 3D bioprinting of heterogeneous aortic valve conduits with alginate/gelatin hydrogels. *J Biomed Mater Res A* 2013; 101: 1255–1264.
62. Ku J, Seonwoo H, Park S, et al. Cell-laden thermosensitive chitosan hydrogel bioinks for 3D bioprinting applications. *Appl Sci* 2020; 10: 2455.
63. Skardal A, Zhang J, McCoard L, et al. Photocrosslinkable hyaluronan-gelatin hydrogels for two-step bioprinting. *Tissue Eng Part A* 2010; 16: 2675–2685.
64. López-Marcial GR, Zeng AY, Osuna C, et al. Agarose-based hydrogels as suitable bioprinting materials for tissue engineering. *ACS Biomater Sci Eng* 2018; 4: 3610–3616.
65. Wu Y, Lin ZY, Wenger AC, et al. 3D bioprinting of liver-mimetic construct with alginate/cellulose nanocrystal hybrid bioink. *Bioprinting* 2018; 9: 1–6.
66. Xin S, Chimene D, Garza JE, et al. Clickable PEG hydrogel microspheres as building blocks for 3D bioprinting. *Biomater Sci* 2019; 7: 1179–1187.
67. Müller M, Becher J, Schnabelrauch M, et al. Nanostructured pluronic hydrogels as bioinks for 3D bioprinting. *Biofabrication* 2015; 7: 035006.
68. Narayanan LK, Huebner P, Fisher MB, et al. 3D-bioprinting of polylactic acid (PLA) nanofiber-alginate hydrogel bioink containing human adipose-derived stem cells. *ACS Biomater Sci Eng* 2016; 2: 1732–1742.
69. Ramasamy S, Davoodi P, Vijayavenkataraman S, et al. Optimized construction of a full thickness human skin equivalent using 3D bioprinting and a PCL/collagen dermal scaffold. *Bioprinting* 2021; 21: e00123.
70. Lee H, Yoo JJ, Kang H-W, et al. Investigation of thermal degradation with extrusion-based dispensing modules for 3D bioprinting technology. *Biofabrication* 2016; 8: 015011.
71. Kundu J, Shim J-H, Jang J, et al. An additive manufacturing-based PCL-alginate-chondrocyte bioprinted scaffold for cartilage tissue engineering. *J Tissue Eng Regen Med* 2015; 9: 1286–1297.
72. Bhattacharjee P and Ahearne M. Significance of crosslinking approaches in the development of next generation hydrogels for corneal tissue engineering. *Pharmaceutics* 2021; 13: 319.
73. GhavamiNejad A, Ashammakhi N, Wu XY, et al. Crosslinking strategies for 3D bioprinting of polymeric hydrogels. *Small* 2020; 16: e2002931.
74. Downie LE, Bandlitz S, Bergmanson JPG, et al. CLEAR - anatomy and physiology of the anterior eye. *Cont Lens Anterior Eye* 2021; 44: 132–156.
75. Marques CF, Diogo GS, Pina S, et al. Collagen-based bioinks for hard tissue engineering applications: a comprehensive review. *J Mater Sci Mater Med* 2019; 30: 32.
76. Gómez-Guillén MC, Giménez B, López-Caballero ME, et al. Functional and bioactive properties of collagen and gelatin from alternative sources: a review. *Food Hydrocolloids* 2011; 25: 1813–1827.
77. Sharifi S, Islam MM, Sharifi H, et al. Tuning gelatin-based hydrogel towards bioadhesive ocular tissue engineering applications. *Bioact Mater* 2021; 6: 3947–3961.
78. Choi DJ, Park SJ, Gu BK, et al. Effect of the pore size in a 3D bioprinted gelatin scaffold on fibroblast proliferation. *J Ind Eng Chem* 2018; 67: 388–395.
79. Laronda MM, Rutz AL, Xiao S, et al. A bioprosthetic ovary created using 3D printed microporous scaffolds restores ovarian function in sterilized mice. *Nat Commun* 2017; 8: 15261.
80. Andersen T, Auk-Emblem P and Dornish M. 3D cell culture in alginate hydrogels. *Microarrays* 2015; 4: 133–161.
81. Axpe E and Oyen ML. Applications of alginate-based bioinks in 3D bioprinting. *Int J Mol Sci* 2016; 17: 1976.
82. Haug A, Smidsrød O, Larsen B, et al. The effect of divalent metals on the properties of alginate solutions. II. Comparison of different metal ions. *Acta Chem Scand* 1965; 19: 341–351.
83. Tabriz AG, Hermida MA, Leslie NR, et al. Three-dimensional bioprinting of complex cell laden alginate hydrogel structures. *Biofabrication* 2015; 7: 045012.
84. Gilbert TW, Sellaro TL and Badylak SF. Decellularization of tissues and organs. *Biomaterials* 2006; 27: 3675–3683.
85. Abaci A and Guvendiren M. Designing decellularized extracellular matrix-based bioinks for 3D bioprinting. *Adv Healthc Mater* 2020; 9: e2000734.
86. Luo Z, Bian Y, Su W, et al. Comparison of various reagents for preparing a decellularized porcine cartilage scaffold. *Am j transl res* 2019; 11: 1417–1427.
87. Croisier F and Jérôme C. Chitosan-based biomaterials for tissue engineering. *Eur Polym J* 2013; 49: 780–792.
88. Kim C-H, Park SJ, Yang DH, et al. Chitosan for tissue engineering. *Adv Exp Med Biol* 2018; 1077: 475–485.
89. Ahearne M, Fernández-Pérez J, Masterton S, et al. Designing scaffolds for corneal regeneration. *Adv Funct Mater* 2020; 30: 1908996.
90. Collins MN and Birkinshaw C. Hyaluronic acid based scaffolds for tissue engineering–a review. *Carbohydr Polym* 2013; 92: 1262–1279.

91. Fitzsimmons TD, Fagerholm P, Härfstrand A, et al. Hyaluronic acid in the rabbit cornea after excimer laser superficial keratectomy. *Investig Ophthalmol Vis Sci* 1992; 33: 3011–3016.
92. Cahill TJ, Sun X, Ravaud C, et al. Tissue-resident macrophages regulate lymphatic vessel growth and patterning in the developing heart. *Development* 2021; 148: dev194563.
93. Xiong J-Y, Narayanan J, Liu X-Y, et al. Topology evolution and gelation mechanism of agarose gel. *J Phys Chem B* 2005; 109: 5638–5643.
94. Fedorovich NE, De Wijn JR, Verbout AJ, et al. Three-dimensional fiber deposition of cell-laden, viable, patterned constructs for bone tissue printing. *Tissue Eng Part A* 2008; 14: 127–133.
95. Shoichet MS, Li RH, White ML, et al. Stability of hydrogels used in cell encapsulation: an in vitro comparison of alginate and agarose. *Biotechnol Bioeng* 1996; 50: 374–381.
96. Ganesh D and Lin SR. Global metrics on ocular biometry: representative averages and standard deviations across ten countries from four continents. *Eye* 2023; 37: 511–515.
97. Fares U, Otri AM, Al-Aqaba MA, et al. Correlation of central and peripheral corneal thickness in healthy corneas. *Cont Lens Anterior Eye* 2012; 35: 39–45.
98. Sridhar MS. Anatomy of cornea and ocular surface. *Indian J Ophthalmol* 2018; 66: 190–194.
99. Meek KM and Knupp C. Corneal structure and transparency. *Prog Retin Eye Res* 2015; 49: 1–49.
100. Knupp C, Pinali C, Lewis PN, et al. The architecture of the cornea and structural basis of its transparency. *Adv Protein Chem Struct Biol* 2009; 78: 25–49.
101. Dyrlund TF, Poulsen ET, Scavenius C, et al. Human cornea proteome: identification and quantitation of the proteins of the three main layers including epithelium, stroma, and endothelium. *J Proteome Res* 2012; 11: 4231–4239.
102. DelMonte DW and Kim T. Anatomy and physiology of the cornea. *J Cataract Refract Surg* 2011; 37: 588–598.
103. Jester JV, Barry PA, Lind GJ, et al. Corneal keratocytes: in situ and in vitro organization of cytoskeletal contractile proteins. *Investig Ophthalmol Vis Sci* 1994; 35: 730–743.
104. Beuerman RW and Pedroza L. Ultrastructure of the human cornea. *Microsc Res Tech* 1996; 33: 320–335.
105. Bourne WM, Nelson LR and Hodge DO. Central corneal endothelial cell changes over a ten-year period. *Investig Ophthalmol Vis Sci* 1997; 38: 779–782.
106. van den Berg TJ and Tan KE. Light transmittance of the human cornea from 320 to 700 nm for different ages. *Vision Res* 1994; 34: 1453–1456.
107. Beems EM and Van Best JA. Light transmission of the cornea in whole human eyes. *Exp Eye Res* 1990; 50: 393–395.
108. Boettner EA and Wolter JR. Transmission of the ocular media. *Investig Ophthalmol Vis Sci* 1962; 1: 776–783.
109. Freegard TJ. The physical basis of transparency of the normal cornea. *Eye* 1997; 11(Pt 4): 465–471.
110. Kling S and Hafezi F. Corneal biomechanics - a review. *Ophthalmic Physiol Opt* 2017; 37: 240–252.
111. Michelacci YM. Collagens and proteoglycans of the corneal extracellular matrix. *Braz J Med Biol Res* 2003; 36: 1037–1046.
112. Hatami-Marbini H and Etebu E. Hydration dependent biomechanical properties of the corneal stroma. *Exp Eye Res* 2013; 116: 47–54.
113. Formisano N, van der Putten C, Grant R, et al. Mechanical properties of bioengineered corneal stroma. *Adv Healthc Mater* 2021; 10: e2100972.
114. Elsheikh A, Alhasso D and Rama P. Biomechanical properties of human and porcine corneas. *Exp Eye Res* 2008; 86: 783–790.
115. Garcia-Porta N, Fernandes P, Queiros A, et al. Corneal biomechanical properties in different ocular conditions and new measurement techniques. *ISRN Ophthalmol* 2014; 2014: 724546.
116. Petsche SJ, Chernyak D, Martiz J, et al. Depth-dependent transverse shear properties of the human corneal stroma. *Investig Ophthalmol Vis Sci* 2012; 53: 873–880.
117. Zeng Y, Yang J, Huang K, et al. A comparison of biomechanical properties between human and porcine cornea. *J Biomech* 2001; 34: 533–537.
118. Kim H, Kang B, Cui X, et al. Light-activated decellularized extracellular matrix-based bioinks for volumetric tissue analogs at the centimeter scale (Adv. Funct. Mater. 32/2021). *Adv Funct Mater* 2021; 31: 2011252.
119. Kivelä T and Uusitalo M. Structure, development and function of cytoskeletal elements in non-neuronal cells of the human eye. *Prog Retin Eye Res* 1998; 17: 385–428.
120. Xuan M, Wang S, Liu X, et al. Proteins of the corneal stroma: importance in visual function. *Cell Tissue Res* 2016; 364: 9–16.
121. Kao WW and Liu C-Y. Roles of lumican and keratocan on corneal transparency. *Glycoconj J* 2002; 19: 275–285.
122. Chen S, Young MF, Chakravarti S, et al. Interclass small leucine-rich repeat proteoglycan interactions regulate collagen fibrillogenesis and corneal stromal assembly. *Matrix Biol* 2014; 35: 103–111.
123. Chen S, Sun M, Iozzo RV, et al. Intracellularly-retained decorin lacking the C-terminal ear repeat causes ER stress: a cell-based etiological mechanism for congenital stromal corneal dystrophy. *Am J Pathol* 2013; 183: 247–256.
124. Bredrup C, Stang E, Bruland O, et al. Decorin accumulation contributes to the stromal opacities found in congenital stromal corneal dystrophy. *Investig Ophthalmol Vis Sci* 2010; 51: 5578–5582.
125. Santhanam A, Torricelli AA, Wu J, et al. Differential expression of epithelial basement membrane components nidogens and perlecan in corneal stromal cells in vitro. *Mol Vis* 2015; 21: 1318–1327.
126. Das SK, Gupta I, Cho YK, et al. Vimentin knockdown decreases corneal opacity. *Investig Ophthalmol Vis Sci* 2014; 55: 4030–4040.
127. Gordon SR. Fibronectin antibody labels corneal stromal collagen fibrils in situ along their length and circumference and demonstrates distinct staining along the cell and stromal interfaces of Descemet's membrane. *Curr Eye Res* 2014; 39: 312–316.

128. Gealy C, Hayes AJ, Buckwell R, et al. Actin and type I collagen propeptide distribution in the developing chick cornea. *Investig Ophthalmol Vis Sci* 2009; 50: 1653–1658.
129. Maurice DM. The structure and transparency of the cornea. *J Physiol* 1957; 136: 263–286.
130. Singh V, Tiwari A, Kethiri AR, et al. Current perspectives of limbal-derived stem cells and its application in ocular surface regeneration and limbal stem cell transplantation. *Stem Cells Transl Med* 2021; 10: 1121–1128.
131. Yang Q, Gao B and Xu F. Recent advances in 4D bioprinting. *Biotechnol J* 2020; 15: e1900086.
132. Castilho M, Levato R, Bernal PN, et al. Hydrogel-based bioinks for cell electrowriting of well-organized living structures with micrometer-scale resolution. *Biomacromolecules* 2021; 22: 855–866.
133. Berg J and Kurreck J. Clean bioprinting - fabrication of 3D organ models devoid of animal components. *ALTEX* 2021; 38: 269–288.
134. Tamminen S and Vermeulen N. Bio-objects: new conjugations of the living. *Sociologias* 2019; 21: 156–179.
135. Rico-Sánchez L, Garzón I, González-Andrades M, et al. Successful development and clinical translation of a novel anterior lamellar artificial cornea. *J Tissue Eng Regen Med* 2019; 13: 2142–2154.
136. Pellegrini G, Ardigò D, Milazzo G, et al. Navigating market authorization: the path holoclar took to become the first stem cell product approved in the European Union. *Stem Cells Transl Med* 2018; 7: 146–154.
137. Herberts CA, Kwa MS and Hermsen HP. Risk factors in the development of stem cell therapy. *J Transl Med* 2011; 9: 29.
138. Sekar MP, Budharaju H, Zennifer A, et al. Current standards and ethical landscape of engineered tissues-3D bioprinting perspective. *J Tissue Eng* 2021; 12: 20417314211027677.